ADAPTIVE IMMUNE SYSTEM

TGFβ prevents IgE-mediated allergic disease by restraining T follicular helper 2 differentiation

Tamara T. Haque[1], Katherine A. Weissler[1], Zoe Schmiechen[1], Karen Laky[1], Daniella M. Schwartz[1], Jenny Li[1], Michela Locci[2], Mathilde Turfkruyer[1], Chen Yao[3], Paul Schaughency[4], Lashawna Leak[1], Justin Lack[4], Yuka Kanno[3], John O'Shea[3], Pamela A. Frischmeyer-Guerrerio[1]*

Allergic diseases are common, affecting more than 20% of the population. Genetic variants in the TGFβ pathway are strongly associated with atopy. To interrogate the mechanisms underlying this association, we examined patients and mice with Loeys-Dietz syndrome (LDS) who harbor missense mutations in the kinase domain of *TGFBR1/2*. We demonstrate that LDS mutations lead to reduced TGFβ signaling and elevated total and allergen-specific IgE, despite the presence of wild-type T regulatory cells in a chimera model. Germinal center activity was enhanced in LDS and characterized by a selective increase in type 2 follicular helper T cells ($T_{FH}2$). Expression of *Pik3cg* was increased in LDS T_{FH} cells and associated with reduced levels of the transcriptional repressor SnoN. PI3Kγ/mTOR signaling in LDS naïve $CD4^+$ T cells was elevated after T cell receptor cross-linking, and pharmacologic inhibition of PI3Kγ or mTOR prevented exaggerated $T_{FH}2$ and antigen-specific IgE responses after oral antigen exposure in an adoptive transfer model. Naïve $CD4^+$ T cells from nonsyndromic allergic individuals also displayed decreased TGFβ signaling, suggesting that our mechanistic discoveries may be broadly relevant to allergic patients in general. Thus, TGFβ plays a conserved, T cell–intrinsic, and nonredundant role in restraining $T_{FH}2$ development via the PI3Kγ/mTOR pathway and thereby protects against allergic disease.

INTRODUCTION

Allergic diseases are a worldwide public health problem (*1*). The generation of immunoglobulin E (IgE) antibodies is a cardinal feature of allergic disorders, yet the mechanisms that regulate IgE production are inadequately understood. A number of genes are linked to atopic conditions including variants in the genes encoding the receptor for transforming growth factor–β (TGFβ) and other genes downstream of TGFβR signaling (*2*–*8*). Variants associated with low TGFβ production are positively correlated with eczema in children, and polymorphisms in *TGFB1* are associated with elevated total IgE levels (*9*, *10*). Furthermore, epidemiologic studies suggest that TGFβ in breast milk may protect against the development of allergic disease, and children with food allergy have diminished TGFβ-producing T cells in their intestinal mucosa (*11*–*13*). Murine studies have also demonstrated that reduced TGFβ expression exacerbates asthma, whereas oral administration of TGFβ suppresses IgE production (*14*–*18*). Collectively, these studies suggest that the TGFβ pathway plays a key role in the pathogenesis of allergy; however, the specific mechanisms involved are largely unknown.

Patients with the rare Mendelian disorder Loeys-Dietz syndrome (LDS) harbor heterozygous loss-of-function mutations in *TGFBR1* or *TGFBR2*. These patients exhibit high levels of allergen-specific and total IgE along with a strong predisposition for allergic disorders, including IgE-mediated food allergy, asthma, allergic rhinitis, eczema, and eosinophilic esophagitis (*19*, *20*). LDS provides a unique opportunity to understand how TGFβ signaling regulates IgE responses with broad relevance to allergic disease in general.

[1]Laboratory of Allergic Diseases, National Institute of Allergy and Infectious Diseases, National Institutes of Health, Bethesda, MD, USA. [2]Department of Microbiology, Perelman School of Medicine, University of Pennsylvania, Philadelphia, PA, USA. [3]Laboratory of Lymphocyte Nuclear Biology, National Institute of Arthritis and Musculoskeletal and Skin Diseases, National Institutes of Health, Bethesda, MD, USA. [4]Collaborative Bioinformatics Resource, National Institute of Allergy and Infectious Diseases, National Institutes of Health, Bethesda, MD, USA.
*Corresponding author. Email: pamela.guerrerio@nih.gov

T follicular helper (T_{FH}) cells are key regulators of humoral immunity that direct B cell proliferation, class switching, and differentiation to antibody-secreting plasma cells and long-lived memory B cells in germinal centers (GCs) (*21*–*23*). Growing evidence in mice and humans indicates that distinct functional subtypes of T_{FH} cells—$T_{FH}1$, $T_{FH}2$, $T_{FH}13$, and $T_{FH}17$ cells—secrete cytokine characteristic of each of the T helper (T_H) effector types and thereby differentially regulate the nature of humoral responses (*24*–*26*). $T_{FH}2$- and $T_{FH}13$-derived interleukin-4 (IL-4) and IL-13 promote class switching to IgE (*26*–*29*). These cells are more abundant in the blood of patients with allergic disease, and their frequency correlates with IgE levels (*24*, *30*, *31*). The pathways that regulate $T_{FH}2$ differentiation are not well understood.

TGFβ and $T_{FH}2$ cells have both been linked to allergic diseases. However, to date, there is no consensus in the literature about how TGFβ influences T_{FH} differentiation. In vivo murine studies have reported both a positive and negative role for TGFβ in driving T_{FH} development (*32*, *33*). Most studies using human cells conclude that TGFβ induces T_{FH} differentiation, based on data from in vitro cultures (*34*, *35*). The role of TGFβ in the differentiation of individual T_{FH} subsets in vivo is also unclear. Given the growing evidence that dysregulated TGFβ signaling is associated with allergic diseases and $T_{FH}2$ cells play an integral role in IgE generation, understanding how TGFβ regulates $T_{FH}2$ cells may inform key mechanisms involved in the development of allergic diseases.

Here, we sought to dissect the role of TGFβ in T_{FH} generation and humoral responses in vivo using samples from patients with LDS and a mouse model of LDS ($Tgfbr1^{WT/mut}$) (*36*). We found that patients with LDS had an increase in total T_{FH} cells that was driven by a selective increase in $T_{FH}2$ cells compared with healthy controls. Furthermore, in both patients with LDS and mice, increased $T_{FH}2$ cells were accompanied by elevated levels of total and food-specific IgE. LDS T cells exhibited enhanced phosphatidylinositol 3-kinase γ (PI3Kγ) expression and activity after T cell receptor (TCR) cross-linking.

Pharmacologic inhibition of PI3Kγ or mammalian target of rapamycin (mTOR) signaling in vivo abrogated the accumulation of food antigen–specific LDS $T_{FH}2$ cells and prevented exaggerated humoral responses in mice in a T cell–intrinsic manner. We further demonstrate that TGFβ-induced Smad2/3 phosphorylation (pSmad2/3) is impaired in nonsyndromic allergic patients' naïve T cells. These findings reveal a conserved role for TGFβ in restraining spontaneous $T_{FH}2$ accumulation in vivo and suggest that impairment in this pathway contributes to enhanced humoral responses including IgE production and the allergic cascade.

RESULTS

TGFβ signaling is impaired in $CD4^+$ T cells from patients with LDS and mice and nonsyndromic allergic patients

Most mutations that cause LDS are missense mutations in the highly conserved kinase domain of *TGFBR1* (type 1 LDS) or *TGFBR2* (type 2 LDS). Mutant LDS TGFβ receptors expressed in human embryonic kidney 293 cells lacking endogenous TGFβ signaling are unable to propagate a signal (*37*, *38*). Because TGFβ signaling has been shown to play a role in the function and/or development of multiple T cell subsets, we sought to examine TGFβ responsiveness in naïve $CD4^+$ T cells from patients with LDS and *Tgfbr1*$^{WT/mut}$ mice (*34*, *35*, *39*), which harbor a heterozygous knock-in allele of an LDS mutation known to cause severe disease in humans (*36*, *40*). After stimulation with recombinant TGFβ1, pSmad2/3, indicative of canonical TGFβ signaling, was induced in T cells from *Tgfbr1*$^{WT/mut}$ mice and patients. Levels of pSmad2/3 were significantly lower in LDS patient $CD4^+$ T cells compared with healthy volunteer (HV) and *Tgfbr1*$^{WT/mut}$ cells compared with controls at the peak of the response (Fig. 1A and fig. S1). To determine whether this pathway was altered more generally in patients with allergic disease, we also analyzed TGFβ signaling in peripheral blood mononuclear cells (PBMCs) from patients with nonsyndromic IgE-mediated food allergy. Naïve $CD4^+$ T cells from nonsyndromic allergic patients also exhibited reduced levels of pSmad2/3 compared with healthy controls after TGFβ stimulation (Fig. 1A). These data indicate that TGFβ signaling is impaired in naïve $CD4^+$ T cells from patients with LDS and *Tgfbr1*$^{WT/mut}$ mice as well as nonsyndromic allergic patients. Thus, diminished TGFβ signaling in $CD4^+$ T cells correlated with atopy.

Increased humoral responses to innocuous antigens in patients with LDS and mice

Consistent with our previous report, patients with LDS had decreased IgM, normal IgA, and increased total serum IgG and IgE compared with levels observed in age-matched HVs (Fig. 1B) (*20*). The majority of patients with LDS had positive specific IgE testing to common environmental and food allergens (table S1) (*20*). *Tgfbr1*$^{WT/mut}$ mice had reduced total serum IgM and increased IgG, IgA, and IgE, indicative of greater isotype class switching compared with their wild-type (WT) littermates (Fig. 1C).The increased total IgG observed was due to a selective increase in IgG1, which is associated with enhanced T_H2 immune responses in mice. In contrast, no significant difference was observed in isotype characteristic of T_H1 responses, namely, IgG2a, IgG2b, or IgG3 (Fig. 1D) (*41*). Analogous to patients with LDS, *Tgfbr1*$^{WT/mut}$ mice became spontaneously sensitized to dietary food antigens as evidenced by elevated levels of IgE specific for wheat, the predominant component of their chow, and this was not observed in mice consuming a wheat-free control diet (Fig. 1E). *Tgfbr1*$^{WT/mut}$ mice orally sensitized with peanut and cholera toxin (a T_H2 adjuvant) developed increased peanut-specific IgE compared with WT controls (Fig. 1F). Immunization with chicken egg ovalbumin (OVA) in Freund's complete adjuvant (FCA; a T_H1 adjuvant) also elicited higher antigen-specific IgE responses in *Tgfbr1*$^{WT/mut}$ mice compared with WT littermates (Fig. 1G). Collectively, these data suggest that diminished TGFβ signaling is associated with increased type 2 humoral immune responses, including total and food antigen–specific IgE production, in both humans and mice.

Increased $T_{FH}2$ cells and GC activity in LDS mice and humans

Mesenteric lymph nodes (mLNs) and Peyer's patches (PP) constitutively harbor GCs because of chronic exposure to food and microbial antigens. Both structures are important sites for the development of oral tolerance, and disruption in this process can lead to food allergy. GCs in PP of *Tgfbr1*$^{WT/mut}$ mice were larger compared with those in WT, although the overall structure and organization of GCs were similar, with distinct T and B cell zones present in both (Fig. 2A). Flow cytometric analyses confirmed that mLN and PP from *Tgfbr1*$^{WT/mut}$ mice exhibited increased frequencies and numbers of GC B cells and class-switched $CD19^+IgD^-$ plasmablasts (Fig. 2B and fig. S2). GC B cell class switching is controlled by T_{FH} cells (*42*), and whereas WT and *Tgfbr1*$^{WT/mut}$ mice had similar numbers of total $CD4^+$ T cells in PP and mLN, activated ($CD44^+$) and T_{FH} ($CXCR5^+PD1^+$) cells were increased in *Tgfbr1*$^{WT/mut}$ mice (Fig. 2, C and D, and fig. S3A). TGFβ is an important regulator of cell proliferation and survival in multiple cell types (*33*, *43*); however, we detected similar frequencies of annexin V and Ki67 staining in WT and *Tgfbr1*$^{WT/mut}$ T_{FH}, indicating that the increase in T_{FH} cells observed in *Tgfbr1*$^{WT/mut}$ mice could not be explained by either reduced apoptosis or greater proliferation (fig. S3B). We found that IL-4–producing T_{FH} cells, which play a critical role in promoting IgE production, were increased in PP, mLN, and spleen in *Tgfbr1*$^{WT/mut}$ mice (Fig. 2, E and F, and fig. S3C). In contrast, the frequency of IL-4^+ T_H2 effector cells was similar in *Tgfbr1*$^{WT/mut}$ and WT mice (Fig. 2E and fig. S3C), indicating a specific increase in $T_{FH}2$ cells. There was no difference in IL-13–producing T_{FH} or non-T_{FH} T cells at steady state or in interferon-γ (IFN-γ)–producing T_{FH} or non-T_{FH} effector cell populations in response to Freund's complete adjuvent (FCA) immunization (fig. S3, D to F). Collectively, these results demonstrate that GC reactions and $T_{FH}2$ cell frequencies are exaggerated in naïve LDS mice, implicating a role for TGFβ in regulating GC reactions and T_{FH} responses to innocuous antigens.

In humans, differential expression of the chemokine receptors CCR4, CXCR3, and CCR6 defines distinct T_{FH} lineages that correspond to the different $CD4^+$ effector T cell populations (*25*). To validate the use of chemokine receptors in defining $T_{FH}1$, $T_{FH}2$, and $T_{FH}17$ cells, we sorted T_{FH} cells on the basis of their expression of the chemokine markers and then determined whether they produced the expected cytokines (Fig. 3A and fig. S4A). As expected, high levels of IFN-γ were detected in $CXCR3^+$ $T_{FH}1$ cells, IL-4 and IL-13 in $CCR4^+$ $T_{FH}2$s, and IL-17 in $CCR6^+$ $T_{FH}17$s (Fig. 3A). Patients with LDS exhibited significantly increased frequencies of circulating memory $CD4^+$ T cells, $CD4^+$ T_{FH} cells, and plasmablasts compared with age-matched healthy controls (Fig. 3, B and C, and fig. S4, A and B). Furthermore, patients with LDS had a selective increase in $T_{FH}2$ cells, whereas $T_{FH}17$ cells were decreased (Fig. 3B

and fig. S4A). Together, these data demonstrate that at steady state, LDS variants lead to an increased frequency of $T_{FH}2$s and enhanced GC activity.

In vitro differentiation conditions for human T_{FH} cells do not fully mimic T_{FH} development in vivo

The presence of increased T_{FH} cells in the blood of patients with attenuated TGFβ signaling was unexpected, given that published studies using human cells have found that TGFβ induces T_{FH} cell differentiation (*34*, *35*). To reconcile these seemingly disparate findings, we cultured naïve $CD4^+$ T cells from patients with LDS or healthy age-matched volunteers in serum-free media supplemented with IL-7, IL-12, and recombinant TGFβ1 as previously described (*34*, *35*). TGFβ enhanced cell surface expression of CXCR5 on cells from healthy individuals (Fig. 3D), consistent with prior reports; however, this was not seen in naïve T cells from patients with LDS, in line with their reduced ability to respond to TGFβ. At the transcriptional level, T_{FH} signature genes *BCL6*, *BATF*, and *MAF* were all induced in culture conditions that included TGFβ, whereas *PRDM1*, which encodes for the strong negative regulator of T_{FH} differentiation Blimp1, was down-regulated (Fig. 3E). Thus, our in vitro studies further confirm that TGFβ promotes T_{FH} differentiation.

In addition to genes common to all T_{FH} subsets, we expanded our analysis to include expression of T_{FH} lineage–specific genes. Cells cultured under these conditions showed expression of T_H17-associated genes such as *RORC*, *RORA*, and *AHR*, as well as T_H1-associated *TBET*, and regulatory T cell (T_{reg})–associated *FOXP3* (Fig. 3E). In contrast, expression of T_H2-associated *GATA3* was absent, as previously reported (*35*). These results suggest that the conditions used for differentiating human T_{FH} cells in vitro support the development of $T_{FH}1$ and $T_{FH}17$ cells but are not permissive for the development of $T_{FH}2$ cells. Thus, we conclude that in vitro conditions do not fully recapitulate the in vivo environment and specifically the conditions needed for $T_{FH}2$ differentiation. In vivo, TGFβ plays a divergent role in regulating the generation of distinct T_{FH} cell subtypes, promoting $T_{FH}1/T_{FH}17$ while suppressing $T_{FH}2$ differentiation.

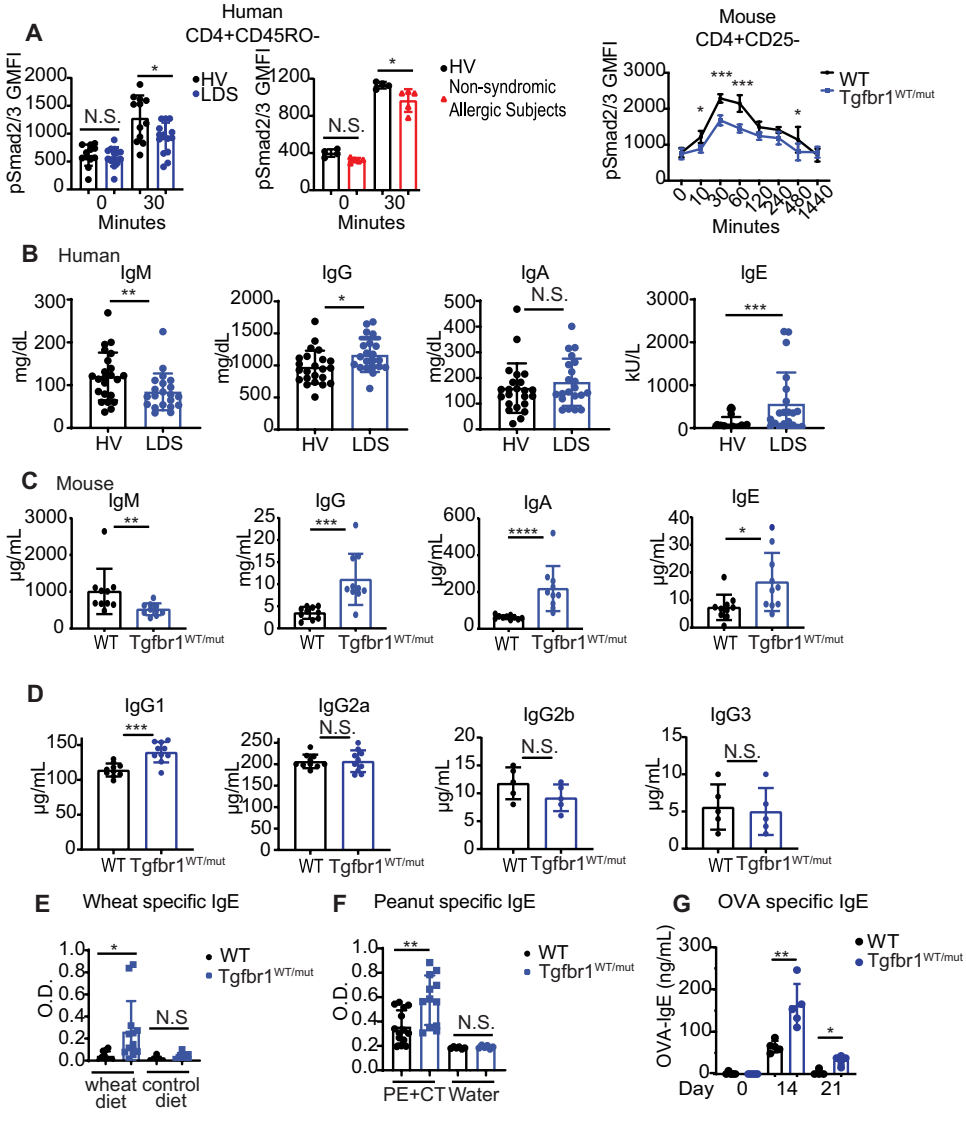

Fig. 1. Reduced canonical TGFβ signaling in T cells is associated with increased serum Igs. (**A**) pSmad2/3 levels in PBMCs from HV, LDS, or nonsyndromic allergic individuals (left) and splenocytes from WT or *Tgfbr1*$^{WT/mut}$ mice (right). Two-way ANOVA with Bonferroni test was used to determine statistical significance for the mouse time course, and Mann-Whitney test was used for the human data. HV $n = 12$, LDS $n = 14$, nonsyndromic allergic individuals $n = 5$ (human) and $n = 5$ (mouse) for each group. (**B**) Serum Ig levels in age-matched HVs and individuals with LDS types 1 and 2. $n = 24$ for HV; $n = 21$ for LDS. A Mann-Whitney test was used to determine statistical significance. (**C** and **D**) Serum Ig levels in WT and *Tgfbr1*$^{WT/mut}$ mice. A Mann-Whitney test was used to determine statistical significance. $n = 10$ for each group. (**E**) Serum from 24-week-old mice was used to measure wheat-specific IgE by ELISA. Statistical significance was determined using a one-way ANOVA followed by Tukey's post hoc test. $n = 10$ (each group) for mice on wheat diet; $n = 6$ (each group) for control diet. (**F**) Peanut-specific IgE was measured in serum by ELISA. $n = 6$ to 11 for each group. A one-way ANOVA followed by Tukey's posttest was used to determine statistical significance. Data are combined from at least two independent experiments. (**G**) OVA-specific IgE in serum was measured by ELISA at the indicated days after OVA immunization. $n = 4$ or 5 mice per group. A Mann-Whitney test was used to determine statistical significance. All experiments were independently performed at least two times. Bar graphs show mean ± SD; $^*P < 0.05$, $^{**}P < 0.01$, $^{***}P < 0.001$, and $^{****}P < 0.0001$. N.S., not significant; GMFI, geometric mean florescence intensity; O.D., optical density. PE, peanut; CT, cholera toxin.

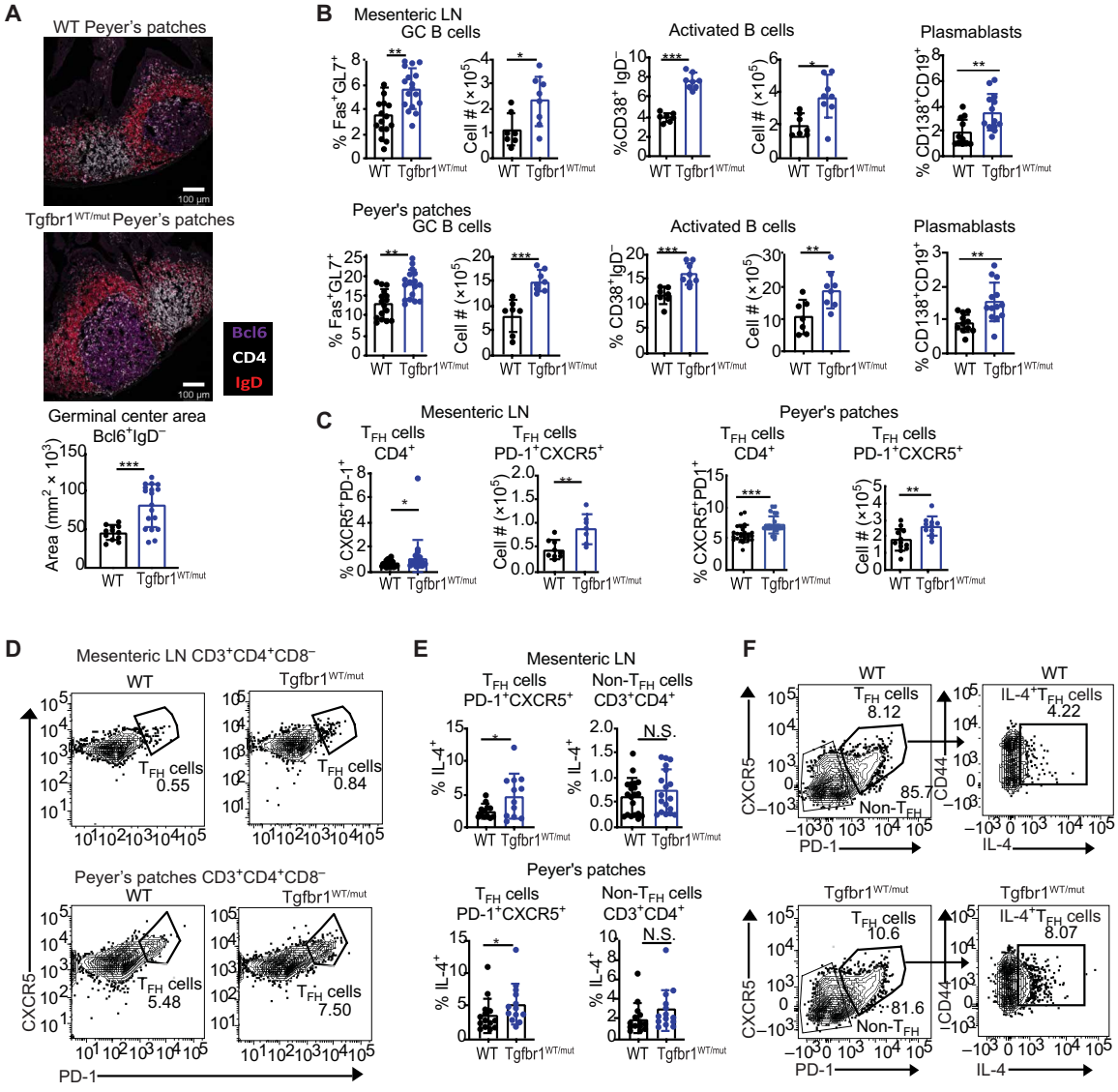

Fig. 2. Increased T_{FH} and GC activity in LDS mice. (**A**) Immunostaining of GCs in murine PP. Image is representative of five WT and five *Tgfbr1*$^{WT/mut}$ mice that were imaged in total. (**B**) Percentage and number of Fas$^+$GL7$^+$ GC B cells and CD38$^+$IgD$^-$ plasmablasts in mouse mLNs and PP. $n = 7$ to 17 per group. (**C**) Number and percentage of T cells expressing CXCR5 and programmed cell death protein (PD-1) in mLN and PP. $n = 8$ to 15 for each group. (**D**) Representative flow cytometry gating for mLN and PP T_{FH} cells. (**E** and **F**) The percentage of IL-4–expressing T_{FH} cells in mLN and PP and representative flow plots. $n = 11$ to 20 per group. All statistical significance was determined using a Mann-Whitney test. Bars represent mean and SEM. Data are combined from at least two independent experiments. *$P < 0.05$, **$P < 0.01$, and ***$P < 0.001$.

Increased $T_{FH}2$ cells and IgE levels in LDS cannot be attributed to T_{reg} dysfunction

TGFβ promotes T_{reg} development and function, and T_{reg} dysfunction has been linked to allergic diseases (*44*–*47*). We therefore sought to determine whether defective T_{regs} contribute to the allergic predisposition in LDS. We found increased numbers of T_{regs} in mLNs of *Tgfbr1*$^{WT/mut}$ mice (Fig 4A), consistent with our previous report that total CD4$^+$ T_{regs} are expanded in the periphery of patients with LDS (*20*). To assess the T_{reg} function, we measured the ability of WT or *Tgfbr1*$^{WT/mut}$ T_{regs} to suppress WT naive CD4$^+$ T cell division in vitro. In the absence of T_{regs}, conventional CD4$^+$ T cells (Tconv) from *Tgfbr1*$^{WT/mut}$ and their WT littermates underwent multiple rounds of division in response to TCR stimulation (Fig. 4B). We found no difference in the ability of WT or *Tgfbr1*$^{WT/mut}$ T_{regs} to inhibit Tconv proliferation in this setting, suggesting that the reduction in TGFβR signaling in LDS does not compromise T_{reg} suppressive function (Fig. 4B). In the converse experiment, *Tgfbr1*$^{WT/mut}$ T cells were efficiently inhibited by WT T_{regs} (Fig. 4B). These results are consistent with our prior report demonstrating normal T_{reg} suppressive activity in patients with LDS (*20*).

We next tested the ability of *Tgfbr1*$^{WT/mut}$ T_{regs} to restrain effector cell activity using an in vivo colitis model whereby CD45RB high effector T cells are transferred into lymphocyte-deficient RAG$^{-/-}$ mice. In the absence of T_{regs}, these cells undergo uncontrolled expansion (Fig. 4, C and D), and this T cell expansion can be suppressed by cotransfer with T_{regs} (*48*, *49*). We found that WT and *Tgfbr1*$^{WT/mut}$

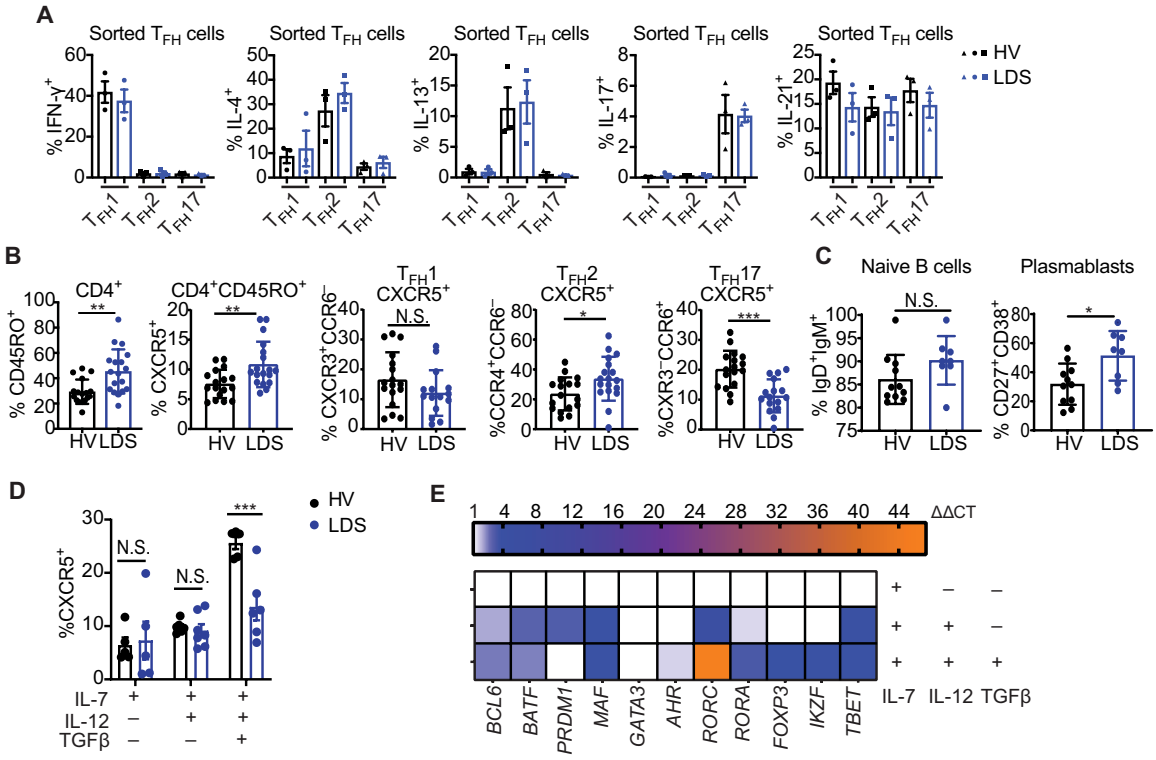

Fig. 3. Patients with LDS have more CD4$^+$ memory T cells, T$_{FH}$2 cells, and plasmablasts ex vivo compared with healthy controls despite reduced T$_{FH}$ differentiation in vitro. (**A**) Intracellular cytokine expression in sorted T$_{FH}$1, T$_{FH}$2, and T$_{FH}$17 cells from HV and patients with LDS. HV $n = 3$; LDS $n = 3$. (**B**) Percentage of CD45RO$^+$ memory cells, total CXCR5$^+$ T$_{FH}$, and T$_{FH}$ lineage subsets in the blood of HVs and patients with LDS. HV $n = 17$; LDS $n = 18$. (**C**) Percentage of circulating naïve B cells and plasmablasts in HVs and patients with LDS . HV $n = 11$; LDS $n = 8$. (**D** and **E**) Naïve CD4$^+$ T cells from patients with LDS or HVs were cultured under the indicated conditions and then analyzed by flow cytometry ($n = 4$ to 6 per group) or (E) HV RNA was collected for qPCR analysis ($n = 3$ to 6). Statistical significance was determined using one-way ANOVA with Tukey's post hoc test for (D) and Mann-Whitney test for all other graphs. Bars represent mean SEM. Data were combined from at least two independent experiments. *$P < 0.05$, **$P < 0.01$,***$P < 0.001$, and not significant $P > 0.05$.

T$_{regs}$ were equally effective at preventing T cell proliferation and effector cytokine production in the mLN and colon lamina propria (Fig. 4, C and D). Collectively, these results demonstrate that *Tgfbr1*$^{WT/mut}$ T$_{regs}$ are as proficient as their WT counterparts at suppressing T effector cell activity; thus, we found no evidence that T$_{reg}$ function is impaired in LDS (*20*).

In contrast to T$_{regs}$, the percentage of T follicular regulatory cells (Tfrs) (CXCR5$^+$Foxp3$^+$), which restrict T$_{FH}$ cell expansion and B cell class switching in GCs (*50*–*53*), was significantly decreased in *Tgfbr1*$^{WT/mut}$ mice and in patients with LDS compared with healthy controls (fig. S5, A and B). Reduced Tfr and enhanced T$_{FH}$ numbers resulted in an increased T$_{FH}$/Tfr ratio in *Tgfbr1*$^{WT/mut}$ mice as compared with WT (fig. S5A). We hypothesized that increased serum IgE in patients with LDS was due to differences in T$_{reg}$ numbers and next tested whether the presence of WT T$_{reg}$ and Tfrs could rescue this phenotype using mixed fetal liver (FL):bone marrow (BM) chimeras (Fig. 4E). In this model, WT or *Tgfbr1*$^{WT/mut}$ FL-derived B cells differentiate in a *Tgfbr1* WT environment and are subject to regulation by WT T$_{regs}$ and Tfrs provided by IgE$^{-/-}$*Tgfbr1*$^{WT/WT}$ BM. Mice reconstituted with *Tgfbr1*$^{WT/mut}$ FL had higher serum IgE than those reconstituted with WT FL cells, despite the presence of WT T$_{regs}$ and equivalent T$_{FH}$:Tfr ratios in mice that received WT and *Tgfbr1*$^{WT/mut}$ FL cells (Fig. 4, F to H). Because the presence of WT T$_{regs}$ and Tfrs cannot suppress the hyper IgE phenotype in LDS, we conclude that exaggerated IgE responses in LDS are independent of T$_{reg}$ and Tfr regulation. Moreover, *Tgfbr1*$^{WT/mut}$ precursors differentiating in a WT environment were more likely to give rise to T$_{FH}$ cells than WT precursors, whereas the total T cell contributions were comparable (Fig. 4I and fig. S6A). Similar changes in T$_{FH}$ frequency were obtained when WT and *Tgfbr1*$^{WT/mut}$ BM was used in place of FL (fig. S6B), confirming that this aspect of the LDS phenotype was hematopoietic cell intrinsic.

T cell–intrinsic changes drive the increase in T$_{FH}$2 cells and allergic sensitization to orally ingested antigens in LDS

To determine whether reduced TGFβ signaling in T cells contributed to the hyper IgE phenotype in LDS in a cell-intrinsic manner, we used a well-established model of oral tolerance. WT or *Tgfbr1*$^{WT/mut}$ OVA-specific OTII T cells were purified and adoptively transferred into CD45.1 congenic WT hosts that were then fed OVA for 7 days (Fig. 5A). On day 8 posttransfer, OVA-specific IgE and IgG1 were significantly higher in the serum of mice receiving *Tgfbr1*$^{WT/mut}$ OTII T cells as compared with recipients of WT OTII T cells (Fig. 5B). These findings indicate that diminished TGFβ signaling in T cells alone is sufficient to enhance class switching to IgG1 and IgE in B cells with intact TGFβ signaling, indicating a T cell–intrinsic phenotype.

To investigate T cell–intrinsic changes resulting from impaired TGFβ signaling, single-cell RNA sequencing (scRNA-seq) analysis

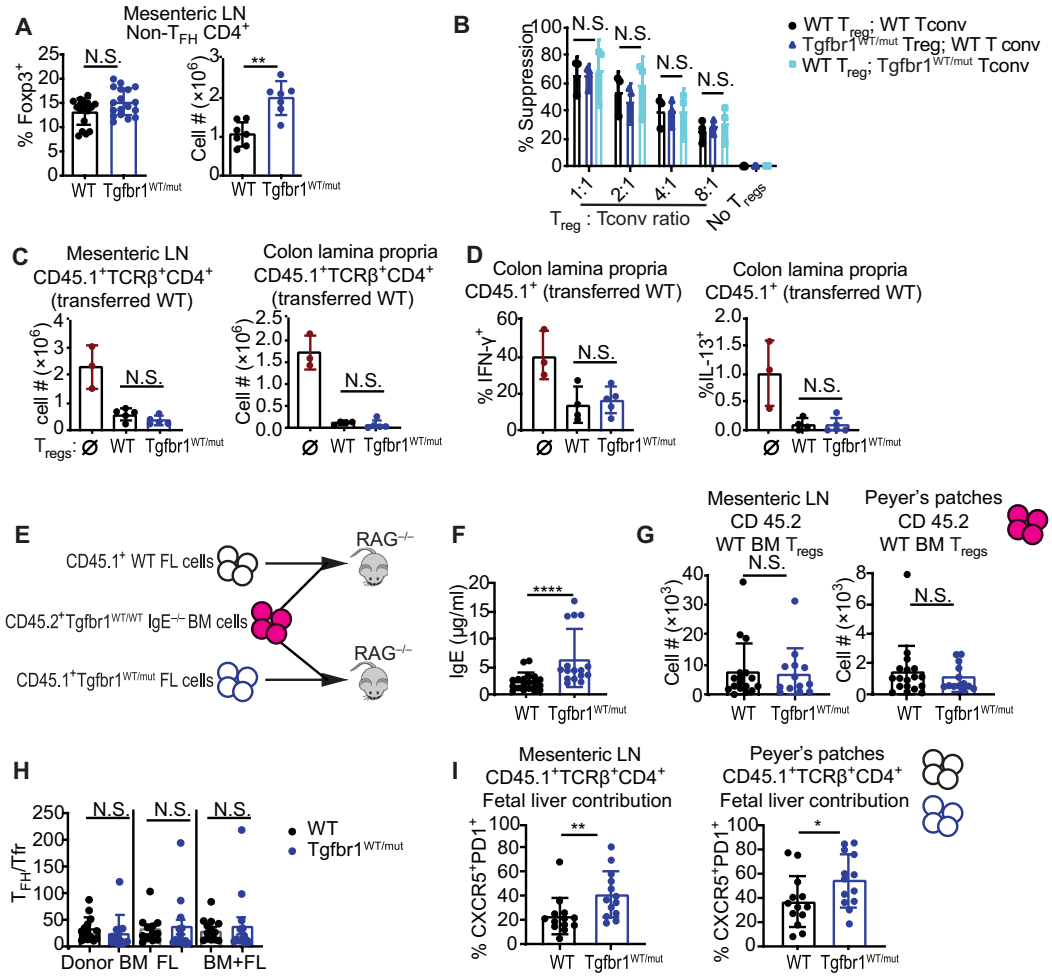

Fig. 4. T$_{regs}$ from *Tgfbr1*$^{WT/mut}$ mice are functional. (**A**) Percentage and number of CD4$^+$ T cells expressing Foxp3 in mLN. $n = 7$ to 18 per group. (**B**) Percent suppression in cultures of naïve CD4$^+$ T cells (T conv) and CD4$^+$CD25$^+$ T$_{regs}$ at indicated ratios. $n = 3$ per group. (**C** and **D**) Accumulation of CD45.1$^+$ (transferred WT T cells) in the mLN and colon lamina propria (LP) and (D) cytokine production by CD45.1$^+$ T cells in the colon LP was determined in a colitis model. $n = 3$ to 5 per group. (**E**) Schematic showing congenically marked BM from IgE knockout (IgE$^{-/-}$) mice mixed 50:50 with 12-day FL cells from WT or *Tgfbr1*$^{WT/mut}$ mice and transferred into sublethally irradiated RAG$^{-/-}$ hosts. (**F**) Total serum IgE after reconstitution. $n = 16$ to 18 per group. (**G**) The WT BM component of Foxp3$^+$CD4$^+$CD45.2$^+$ T$_{reg}$ numbers are shown from the mLNs and PP of hosts. (**H**) Ratio of T$_{FH}$:Tfrs derived from BM, FL, or both combined in the mLN. (**I**) Proportion of CD4$^+$ T cells expressing CXCR5 and PD-1 that were FL derived (G to I, $n = 13$ to 17 per group). A Mann-Whitney test was used to determine statistical significance in all experiments. Bars represent mean and SE. Data are combined from at least two independent experiments. *$P < 0.05$, **$P < 0.01$, and ****$P < 0.0001$.

was performed on OTII cells reisolated from the PP of hosts after 1 week of OVA water consumption. Unbiased clustering revealed five distinct populations (Fig. 5C and fig. S7). *Tgfbr1*$^{WT/mut}$ PP were enriched for the early memory T cells (EMTC) and T$_{FH}$ clusters, indicating that T cells with reduced TGFβ signaling undergo greater activation and antigen-induced T$_{FH}$ differentiation than WT T cells (Fig. 5C). Furthermore, total CD4$^+$ OTII *Tgfbr1*$^{WT/mut}$ cells were enriched for cells with high expression of T$_{FH}$ genes *Bcl6*, *Tox2*, *Cxcr5*, and *Il-21* (Fig. 5D). Flow cytometry analysis of mLNs and PP revealed that *Tgfbr1*$^{WT/mut}$ OTII T cells accumulated more than WT in response to ingested OVA (Fig. 5E). A higher percentage and number of *Tgfbr1*$^{WT/mut}$ OTII cells differentiated into CXCR5$^+$ T$_{FH}$ cells than WT OTII T cells (Fig. 5F), validating the scRNA-seq findings. Specifically, we found increased IL-4–producing T$_{FH}$2 cells in *Tgfbr1*$^{WT/mut}$ recipients (Fig. 5G). Thus, reduced TGFβ signaling in T cells alone replicated the steady-state phenotypes observed in LDS mice and humans, specifically increased T$_{FH}$2 and food-specific serum IgE. Together, these data demonstrate that TGFβ is an essential and nonredundant regulator of T$_{FH}$2 differentiation in the gut and that CD4$^+$ T cells that fail to receive sufficient TGFβ signaling drive sensitization to dietary antigen in a T cell–intrinsic manner.

LDS variants promote dysregulation of the PI3Kγ/mTOR signaling pathway

To probe the mechanisms by which attenuated TGFβ signaling in T cells leads to enhanced T$_{FH}$ differentiation, we sorted total T$_{FH}$ cells from the PP of unmanipulated *Tgfbr1*$^{WT/mut}$ and WT littermates and performed bulk RNA-seq analysis. We found that 240 genes were up-regulated and 228 genes were down-regulated in *Tgfbr1*$^{WT/mut}$ T$_{FH}$ cells compared with WT (fig. S8A and data file S1). Many of the differentially expressed genes overlapped with those previously found to be dysregulated in Smad3-deficient CD4$^+$ T cells treated with

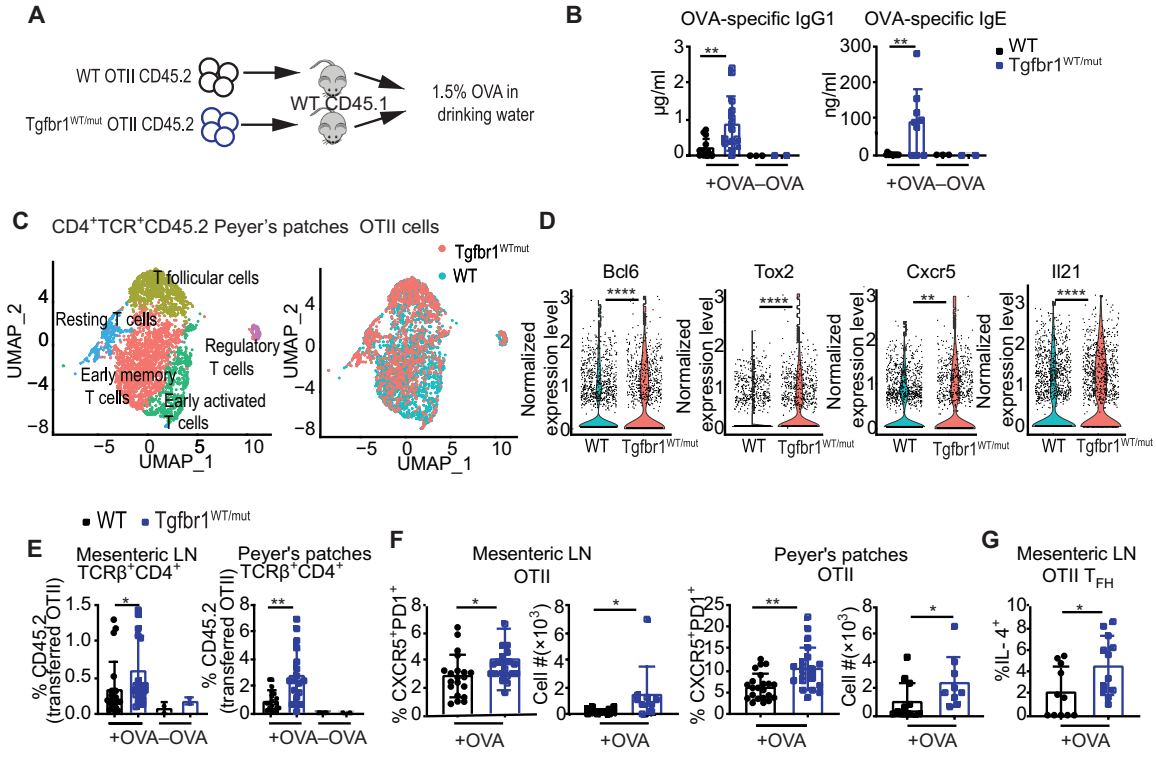

Fig. 5. Increased propensity for naïve CD4$^+$ T cells with the *Tgfbr1* mutation to differentiate into T_{FH} cells and promote IgE production by WT B cells in response to orally delivered food antigen. (**A**) Schematic showing the transfer of WT or *Tgfbr1*$^{WT/mut}$ OTII$^{+/-}$RAG$^{-/-}$ T cells to WT recipients on day 0. Recipient mice were provided with drinking water containing 1.5% OVA starting on day 1 and were analyzed on day 8. (**B**) OVA-specific IgG1 and IgE levels in the serum of recipient mice. $n = 12$ per group. Mann-Whitney test was used to determine statistical significance. (**C**) OTII cells from PP were reisolated from the WT host, and scRNA-seq was performed. Subsets were clustered into resting T cells, T_{reg}, EMTC, T_{FH} cells, and early activated T cells. (**D**) Expression levels for selected T_{FH}-associated genes. (**E**) Transferred CD4$^+$CD3$^+$ OTII cells were identified by expression of CD45.2. (+OVA $n = 20$; −OVA $n = 2$ per group). (**F**) Frequency and number of WT and *Tgfbr1*$^{WT/mut}$ OTII cells in the mLN and PP with a T_{FH} phenotype (CXCR5$^+$PD-1$^+$). $n = 9$ to 22 per group. (**G**) IL-4–producing T_{FH} cells in the mLN were analyzed after restimulation. $n = 11$ or 12 per group. Mann-Whitney test was used to determine statistical significance. Bars represent mean and SE. (C) and (D) are from a single experiment. (B) and (E) to (G) are combined from at least three independent experiments. *$P < 0.05$, **$P < 0.01$, and ****$P < 0.0001$. UMAP, Uniform Manifold Approximation and Projection.

TGFβ, including *Smad7*, *Sardh*, *Ctsw*, *Rgs10*, *Apol9a/b*, *Ctnna1*, *Skil*, and *Kras* (Fig. 6A) (*54*). Furthermore, genes directly induced by Smad3, such as *Skil*, were significantly enriched in WT T_{FH} cells compared with the *Tgfbr1*$^{WT/mut}$ T_{FH} as determined by gene set enrichment analysis (GSEA), consistent with a partial loss-of-function phenotype in LDS T_{FH} cells at the transcriptional level (Fig. 6B and data file S2). Using publicly available datasets (*55*), we found that genes more highly expressed in T_{FH} cells than non-T_{FH} T cells were significantly enriched in *Tgfbr1*$^{WT/mut}$ T_{FH} cells compared with WT T_{FH} cells (Fig. 6C and data file S3). Together, these data illustrate that a partial loss of TGFβ signaling leads to an enhanced T_{FH} transcriptional signature, indicating a fundamental role for TGFβ signaling in T_{FH} cells at steady state.

Ingenuity pathways analysis (IPA) of genes differentially expressed between WT and *Tgfbr1*$^{WT/mut}$ T_{FH} cells revealed a state of increased activation and T_H2 skewing in T_{FH} cells from LDS mice compared with their littermates (Fig. 6D). IL-4 signaling and IL-4 itself, T_H2 pathway, and T_H1 and T_H2 activation pathway were up-regulated in T_{FH} cells isolated from *Tgfbr1*$^{WT/mut}$ mice relative to WT littermates (Fig. 6, D and E). The increase in IL-4 expression was confirmed by quantitative polymerase chain reaction (qPCR) (Fig. 6F).

The most significantly up-regulated gene set in *Tgfbr1*$^{WT/mut}$ versus WT T_{FH} cells identified by IPA analysis was the PI3K pathway (Fig. 6, D and E). PI3Ks are a family of lipid kinases that activate diverse signaling cascades, including the multiprotein complexes containing the serine/threonine kinase mTOR (mTORC1 and mTORC2). *Tgfbr1*$^{WT/mut}$ T_{FH} also featured up-regulation of the p70S6 signaling pathway, which is activated downstream of PI3K/mTOR (Fig. 6D), as well as enrichment of Raptor- and Rictor-dependent genes that are dependent on expression of mTORC1/2 components (Fig. 6G and data file S4). Collectively, these data indicate enhanced PI3K/mTOR signaling in *Tgfbr1*$^{WT/mut}$ T_{FH} cells and up-regulation of downstream pathways previously established to be essential for T_{FH} development.

In particular, *Pik3cg* was up-regulated in *Tgfbr1*$^{WT/mut}$ PP T_{FH} cells compared with WT (Fig. 6E), which was verified by qPCR (Fig. 6F). *Pik3cg* encodes the protein p110γ, which, together with p85, forms PI3Kγ. PI3Kγ signaling is critical in human and mouse T cell function (*56*–*59*). Using publicly available human chromatin immunoprecipitation sequencing data, we found that the *PIK3CG* locus contains two binding sites for SnoN, which is encoded by *SKIL* (fig. S8C). The transcriptional repressor SnoN is induced by TGFβ (*60*–*62*). Thus, TGFβ has the potential to negatively regulate PI3Kγ expression indirectly via SnoN. *Skil* was expressed at lower levels in

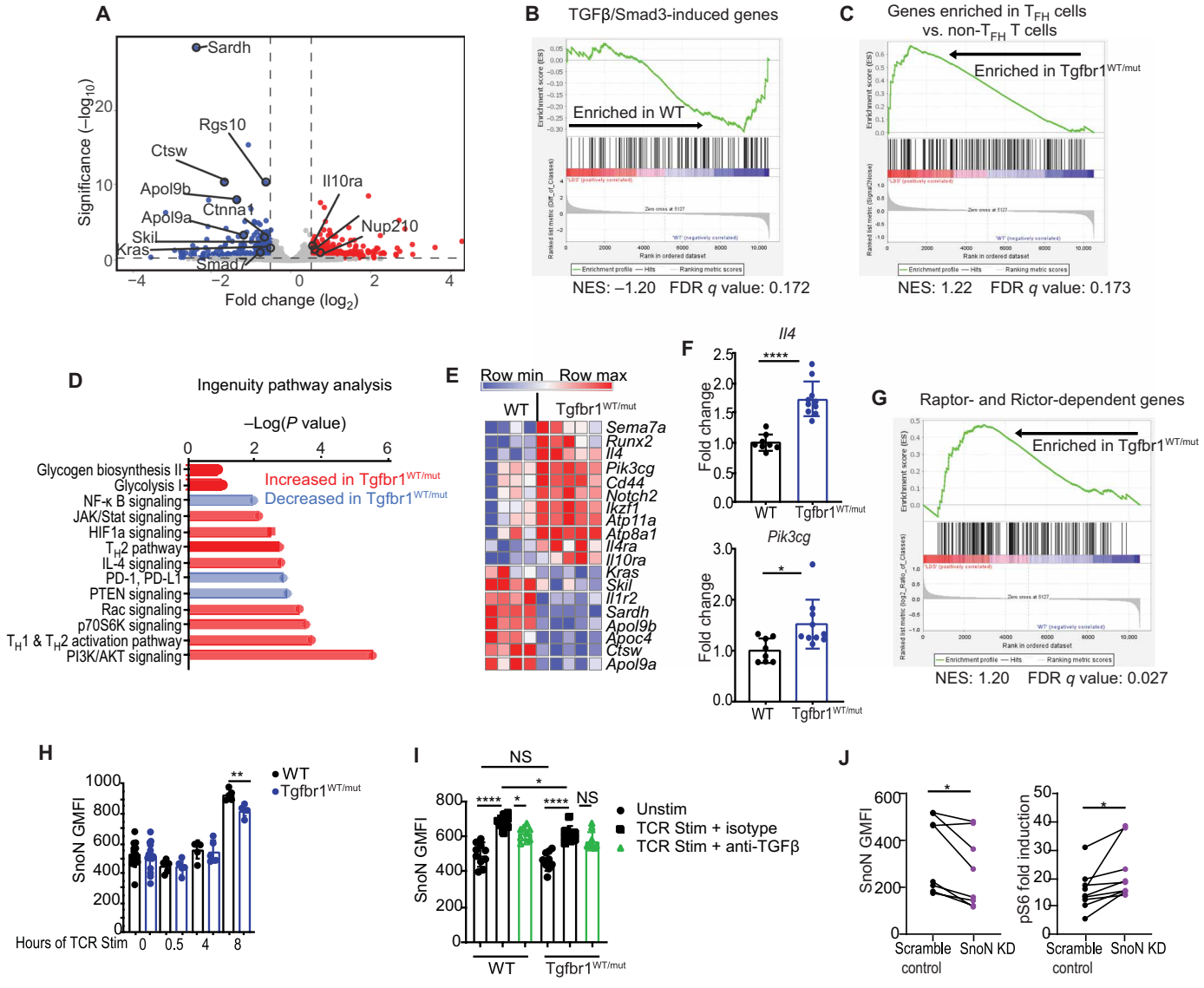

Fig. 6. Enhanced PI3Kγ/mTOR activity in *Tgfbr1*$^{WT/mut}$ T_{FH} cells. WT or *Tgfbr1*$^{WT/mut}$ PP T_{FH} cells were sorted and analyzed by bulk RNA-seq. WT $n = 4$; *Tgfbr1*$^{WT/mut}$ $n = 5$. (**A**) Volcano plot of differentially expressed genes. Labeled genes represent TGFβ-SMAD3–responsive genes with a FDR value of <0.1. (**B**) GSEA of TGFβ-SMAD3–responsive genes (GSE40494). (**C**) GSEA analysis of genes up-regulated in T_{FH} cells compared with non-T_{FH} T cells (GSE21380). (**D**) IPA was performed on the RNA-seq data. Red indicates increased activity in *Tgfbr1*$^{WT/mut}$ T_{FH} cells, and blue indicates decreased activity in *Tgfbr1*$^{WT/mut}$ compared with WT. NF-κB, nuclear factor κB. (**E**) Heatmap of top genes contributing to the pathway analysis results in (D). (**F**) Quantitative PCR for the *Il4* and *Pik3cg* genes on sorted murine PP T_{FH} cells. Statistical significance was determined using Mann-Whitney test. (**G**) GSEA analysis using the genes down-regulated in Raptor- and Rictor-deficient T cells from GSE85555. (**H** and **I**) SnoN expression after TCR stimulation of PP naïve CD4$^+$ T cells [with isotype or anti-TGFβ antibody in (I)] (H, $n = 4$ or 5 per group; I, $n = 9$ or 10 per group). Mann-Whitney test was used to determine statistics in (H). One-way ANOVA, Šidák's test was used to determine statistics in (I). (**J**) SnoN and pS6 expression in WT murine splenic CD4$^+$ T cells transfected with scramble control or *Skil*/SnoN-specific siRNA (SnoN KD). $n = 8$. Statistical significance was determined by paired Student's *t* test. (A) to (G) are from a single experiment, and (H) to (J) are combined from two independent experiments. *$P < 0.05$, **$P < 0.01$, and ****$P < 0.0001$. Bars represent mean and SE. FDR < 0.25 was considered statistically significant for GSEA analysis. NES, normalized enrichment score; PD-L1, programmed death-ligand 1; PTEN, phosphatase and tensin homolog.

Tgfbr1$^{WT/mut}$ than WT T_{FH} ex vivo (Fig. 6, A and E). Moreover, *Skil* levels were also lower in adoptively transferred *Tgfbr1*$^{WT/mut}$ OTII T_{FH} cells recently stimulated by OVA (fig. S8B). However, it was expressed equally in rested naïve CD4$^+$ T cells from PP of WT and *Tgfbr1*$^{WT/mut}$ mice (Fig. 6H). This suggested that altered expression of *Skil* in *Tgfbr1*$^{WT/mut}$ mice was T cell intrinsic and potentially dependent on antigen exposure. To determine the kinetics of SnoN up-regulation after TCR stimulation, naïve CD4$^+$ T cells isolated from PP were rested and then TCR-stimulated in vitro. No significant increase in SnoN expression was observed at 30 min or 4 hours, but expression was significantly higher compared with baseline in both WT and *Tgfbr1*$^{WT/mut}$ cells after 8 hours of stimulation

(Fig. 6H). This difference in expression was at least partially dependent on TGFβ because treatment with a TGFβ-neutralizing antibody reduced SnoN induction at 8 hours (Fig. 6I), such that levels of SnoN in WT cells were similar to those observed in *Tgfbr1*$^{WT/mut}$ cells (Fig. 6J). Collectively, these data show that SnoN is induced by TGFβ during the late phase of TCR activation in CD4$^+$ T cells.

To determine whether reduced expression of SnoN could have functional consequences on PI3K activity, phosphorylation of the downstream signaling molecule S6 in response to TCR cross-linking was evaluated in WT T cells after small interfering RNA (siRNA)–mediated *Skil*/SnoN knockdown (KD). SnoN KD resulted in increased pS6, revealing that SnoN is a negative regulator of this pathway (Fig. 6J). This recapitulated the bulk RNA-seq data showing decreased *Skil* and increased p70S6K signaling coincides in *Tgfbr1*$^{WT/mut}$ T_{FH} cells (Fig. 6, D and E). Together, these findings suggest that in the late phase of TCR activation, TGFβ controls PI3Kγ/mTOR signaling at least in part by inducing SnoN, a transcriptional repressor of *Pik3cg*. In LDS, impaired TGFβR signaling leads to reduced expression of SnoN and less efficient repression of *Pik3cg*, ultimately resulting in enhanced mTOR-mediated signaling downstream of TCR.

TGFβ targets PI3Kγ/mTOR signaling to prevent aberrant T_{FH} accumulation in vivo

To confirm that PI3Kγ/mTOR signaling was dysregulated in LDS, we evaluated PI3K signaling in a constitutively active lymphoid tissue, namely, PP. Expression of both pS6 and pFOXO1 were increased in *Tgfbr1*$^{WT/mut}$ PP T_{FH}, although pFoxO1 was not statistically significant (fig. S9A). To evaluate the kinetics of PI3K signaling in *Tgfbr1*$^{WT/mut}$ and WT PP naïve CD4$^+$ T cells after TCR cross-linking, we measured pS6 and pFoxO1 at different time points after stimulation. Expression of pS6 increased at 0.5 and 4 hours, but levels did not differ between WT and *Tgfbr1*$^{WT/mut}$ (fig. S9B), consistent with equivalent expression of SnoN in WT and *Tgfbr1*$^{WT/mut}$ cells at these time points (Fig. 6H). At 24 hours, however, the percentage of cells expressing pS6 and pFoxO1 was significantly higher in *Tgfbr1*$^{WT/mut}$ relative to WT littermates (Fig. 7A and fig. S9C). Similarly, the

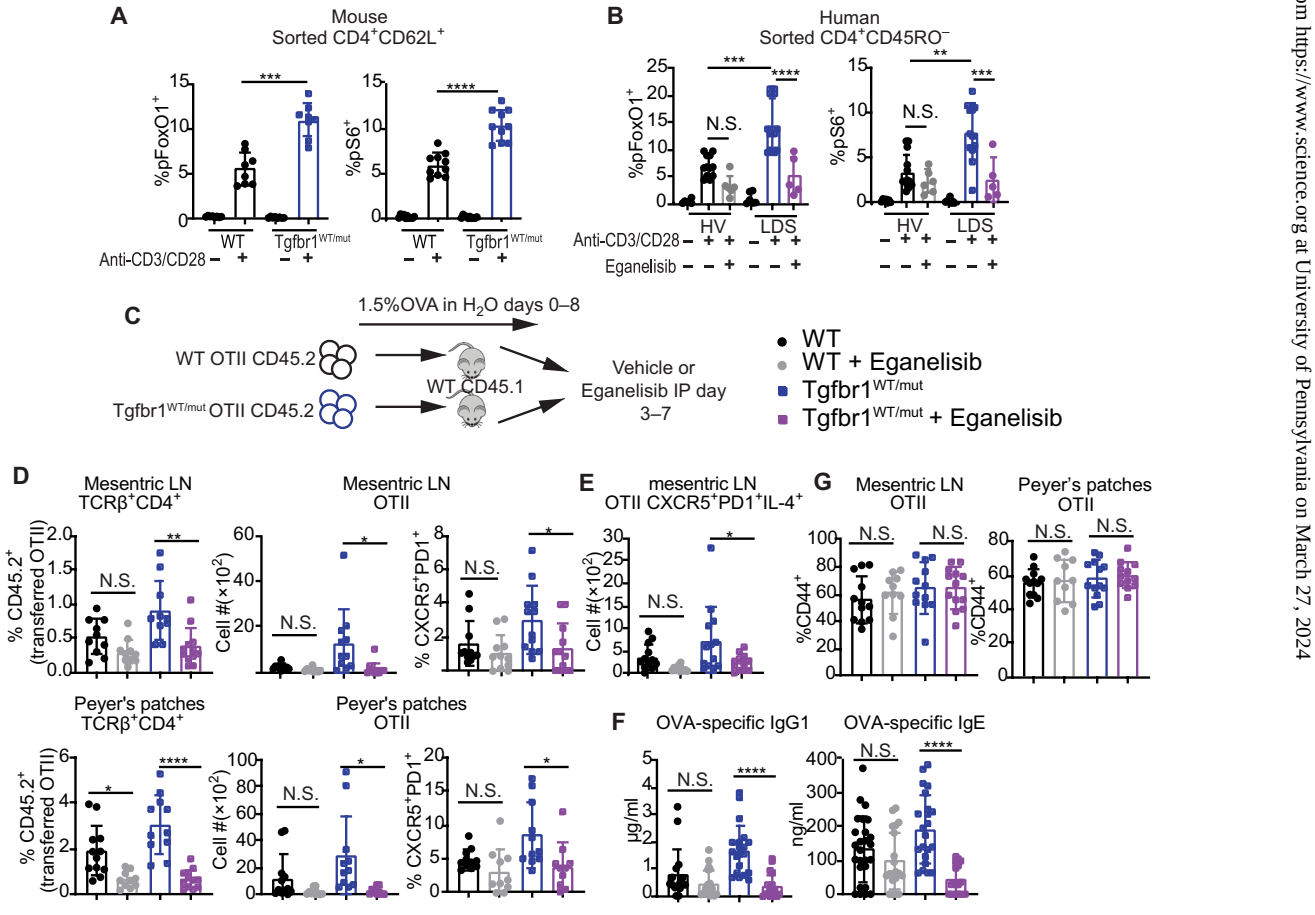

Fig. 7. Inhibition of the PI3Kγ/mTOR pathway prevents excessive generation of LDS T_{FH} cells in response to fed antigen. (**A**) Naïve T cells from murine PP were TCR-stimulated ($n = 6$ per group), and (**B**) naïve human T cells were pretreated with eganelisib or vehicle, TCR-stimulated. Phosphorylation of S6 (pS6) and FoxO1 (pFoxO1) was determined by flow cytometry. HV pS6 $n = 10$, pFoXO1 $n = 6$; LDS pS6 $n = 12$, pFoxO1 $n = 6$. (**C**) WT or *Tgfbr1*$^{WT/mut}$ OTII$^{+/-}$RAG$^{-/-}$ T cells were transferred into WT recipients on day 0. Recipient mice were provided with drinking water containing 1.5% OVA starting on day 0, intraperitoneally (IP) injected with vehicle or eganelisib on days 3 to 7, and then analyzed on day 8. (**D**) Percentage and number of total OTII cells (CD45.2$^+$TCRβ$^+$CD4$^+$) and T_{FH} (CD45.2$^+$CXCR5$^+$PD-1$^+$) cells. $n = 9$ to 11 per group. (**E**) Number of IL-4–producing T_{FH} cells. $n = 11$ to 13 per group. (**F**) OVA-specific IgE and IgG1 levels. $n = 16$ to 24. (**G**) Frequency of CD4$^+$CD44$^+$ memory OTII cells. $n = 9$ or 10 per group. One-way ANOVA, Tukey's test was used to determine statistical significance. Bars represent mean and SEM. All panels depict combined data from two to three independent experiments *$P < 0.05$, **$P < 0.01$,***$P < 0.001$, and ****$P < 0.0001$.

frequency of pS6$^+$ and pFoxO1$^+$ CD4$^+$ T cells was elevated in patients with LDS compared with age-matched healthy controls after 68 hours but not 0.5 hours of anti-CD3/CD28 stimulation (Fig. 7B and fig. S9, B and D). Pharmacological inhibition of PI3Kγ in LDS patient T cells corrected expression of pS6 and pFoxO1 to levels observed in HV T cells (Fig. 7B and fig. S9E). Collectively, our results suggest that TGFβ's inhibitory effect on PI3Kγ/mTOR signaling occurs during the late phase of TCR activation in CD4$^+$ T cells and that the kinetics of this regulation correlates with reduced levels of SnoN in *Tgfbr1*$^{WT/mut}$ after TCR stimulation.

Multiple soluble factors are induced in the late phases of TCR activation that may influence T_{FH} differentiation, including IL-2, which has been shown to be regulated by TGFβ (*63*). To determine whether IL-2 was responsible for the increased late-phase PI3K signaling in *Tgfbr1*$^{WT/mut}$ cells, we performed an IL-2 cytokine capture assay and intracellular IL-2 staining after TCR or phorbol 12-myristate 13-acetate (PMA)/ionomycin stimulation of naïve CD4$^+$ T cells, respectively. No difference in IL-2$^+$ T cells was observed between WT and *Tgfbr1*$^{WT/mut}$ (fig. S9, F and G), suggesting that secondary PI3K signaling induced by IL-2 was an unlikely explanation. To determine whether other secreted factors were responsible, we mixed congenically marked WT:WT or WT:*Tgfbr1*$^{WT/mut}$ PP CD4$^+$ naïve T cells and stimulated them with anti-CD3/CD28 for 24 hours. Under these conditions, *Tgfbr1*$^{WT/mut}$ cells continued to exhibit increased PI3K signaling relative to their WT counterparts, suggesting that an intrinsic factor rather than a soluble mediator(s) drives the increased late-phase PI3K signaling in *Tgfbr1*$^{WT/mut}$ T cells (fig. S9H).

We next investigated whether inhibition of the PI3Kγ/mTOR pathway in vivo could prevent the exaggerated generation of *Tgfbr1*$^{WT/mut}$ T_{FH} cells after antigen exposure. WT or *Tgfbr1*$^{WT/mut}$ OTII cells were transferred into CD45.1 congenic WT hosts, and OVA was added to their drinking water for 8 days. Hosts also received intraperitoneal injection of the PI3Kγ inhibitor eganelisib or vehicle control alone on days 3 to 7 (Fig. 7C). Analysis on day 8 revealed that inhibition of PI3Kγ significantly suppressed the accumulation of OVA-specific *Tgfbr1*$^{WT/mut}$ T_{FH} cells and, in particular, IL-4–producing T_{FH} cells in response to ingested OVA and abrogated the production of OVA-specific IgG1 and IgE (Fig. 7, D to F). The overall early memory response was intact after eganelisib treatment, as determined by the presence of equivalent CD44$^+$ T cells (Fig. 7G). Similar results were obtained after treatment with the mTOR inhibitor rapamycin (fig. S10). Together, our findings suggest that TGFβ is an essential regulator of $T_{FH}2$ differentiation by targeting the PI3Kγ/mTOR pathway in T cells, disruption of which leads to aberrant $T_{FH}2$ differentiation and allergic sensitization to food antigens.

DISCUSSION

Although a complete loss of TGFβ signaling causes severe autoimmunity and death at an early age in murine models, the in vivo consequences of impaired TGFβ signaling in humans is less clear, because most information has relied on in vitro systems. TGFβ signaling is tightly regulated; thus, a complete loss of function may not accurately reflect the clinical consequences of a partial loss caused by genetic variants. Multiple studies point to TGFβ as a key player in allergic diseases, and variants in the TGFβ pathway are associated with allergic conditions in humans. Here, we demonstrate that a modest reduction in canonical TGFβ signaling via pSmad2/3 results in transcriptional changes in T cells that are linked to greater $T_{FH}2$ expansion and enhanced IgE production. We further show that canonical TGFβ signaling is impaired in naïve CD4$^+$ T cells isolated from nonsyndromic food allergic patients compared with age-matched healthy controls, suggesting a role for this signaling pathway in allergic disorders in the general population. Although the pathogenesis of allergic diseases is multifactorial, these findings suggest that perturbations in TGFβ signaling, whether induced by genetic or environmental factors, may contribute to the allergic diathesis in at least a subset of patients (*64*, *65*). By studying patients and mice with a single gene defect leading to partially attenuated canonical TGFβ signaling, we demonstrate that the primary immunological clinical manifestation of reduced TGFβ signaling is an increased propensity for IgE-mediated allergic disease caused by an inability to restrain constitutive $T_{FH}2$ cell activity and IgE production via the PI3Kγ/mTOR pathway in a T cell–intrinsic manner. Our work therefore reveals TGFβ to be a nonredundant, central regulator of T_{FH} cell biology in vivo in both mice and humans and provides a mechanism by which disruption in the TGFβ signaling pathway can contribute to the pathogenesis of allergic disease.

The role of TGFβ in T_{FH} generation has been controversial. In humans, TGFβ in combination with IL-23 or IL-12 promoted the acquisition of T_{FH} properties by naïve CD4$^+$ T cells in vitro, including expression of CXCR5, Bcl6, and CXCL13 (*34*, *35*). Murine models have demonstrated a critical role for TGFβ in T_{FH} generation in vivo, albeit with conflicting conclusions as to whether TGFβ promotes or inhibits T_{FH} development (*32*, *33*). In one study, complete impairment of TGFβ signaling prompted reduced differentiation of viral-specific T_{FH} cells as a result of enhanced CD25 expression and IL-2 signaling after viral challenge (*32*). In a second study, the absence of TGFβ signaling in T cells led to the spontaneous accumulation of T_{FH} cells, autoantibody production, and immune complex deposition (*33*). These incongruities may reflect different pathways for T_{FH} development in response to infectious insults versus homeostatic conditions, as well as heterogeneity in the T_{FH} population. Consistent with previous reports, we found that naïve CD4$^+$ T cells from patients with LDS, who exhibit reduced canonical TGFβ signaling, were less likely to acquire T_{FH} properties in response to TGFβ + IL-12 compared with healthy controls. However, T_{FH} cells were more abundant in the peripheral blood of patients with LDS, and this was coincident with higher levels of IgG and IgE. Although these results appear paradoxical, the increased T_{FH} cells in patients with LDS were specifically of the $T_{FH}2$ subset, whereas $T_{FH}17$ cells were significantly reduced. Thus, the most frequently used in vitro T_{FH} skewing conditions, which are optimized for $T_{FH}1$/$T_{FH}17$ development, do not adequately recapitulate the full range of T_{FH} subsets that are generated in vivo. Genes typically expressed by $T_{FH}17$/$T_{FH}17$ cells were increased under these in vitro conditions, whereas expression of T_H2/$T_{FH}2$-associated genes was absent. Thus, our finding that TGFβ plays a divergent role in the development of T_{FH} subtypes provides a potential explanation for the apparent disparity in prior studies. Moreover, our human and mouse parallel studies demonstrate a critical T cell–intrinsic role for TGFβ in limiting $T_{FH}2$ differentiation in vivo that is conserved across species.

Although a modest increase in IgG is likely to be clinically silent, even small increases in IgE can have clinical consequences because of the extreme sensitivity of IgE allergen recognition. Total and food-specific IgEs were spontaneously increased in patients with LDS and mice, and we found that experimentally LDS mice generated antigen-specific IgE in response to immunization with both

T_H1 and T_H2 adjuvants. Our findings, therefore, inform the mechanisms responsible for the high rate of IgE-mediated diseases in patients with LDS and support recent studies that indicate that T_{FH} cells are key players in IgE-mediated allergic conditions (*66*, *67*). This study also provides additional evidence for the association of genetic variants in the TGFβ pathway with allergic disease and reveal a crucial role for T cell–intrinsic TGFβ signaling in preventing aberrant T_{FH} and GC activity that can lead to IgE-mediated pathology. An increase in IgA in LDS mice was somewhat unexpected because TGFβR signaling in B cells was reported to be essential for IgA generation (*68*, *69*). However, there is evidence that IgA induction can occur independently of TGFβR signaling (*69*). Alternatively, the amount of residual TGFβ signaling in LDS may be sufficient to support IgA production.

Tfrs limit the activity of T_{FH} cells and suppress GC reactions (*70*). Although the frequency of Tfrs was reduced in patients with LDS and mice compared with controls, a deficiency in Tfrs is unlikely to solely account for the expansion of T_{FH} cells in LDS. LDS T_{FH} cells accumulated even in the presence of WT Tfrs in mixed chimera experiments. We further found no evidence for T_{reg} functional defects in LDS mice. Although other hematopoietic cells may contribute to the allergic phenotype in LDS, mixed chimera and OTII adoptive transfer experiments established that T cell–intrinsic changes account for the spontaneous accumulation of T_{FH} cells and exaggerated humoral responses when TGFβ signaling in $CD4^+$ T cells is impaired. Furthermore, we found more IL-4–producing T_{FH} cells in LDS mice, indicating that, in addition to being increased in number, they favor a $T_{FH}2$ phenotype.

Our work demonstrates that one mechanism by which TGFβ regulates T_{FH} development and function involves limiting late phase PI3Kγ/mTOR signaling downstream of TCR. Prior studies found that T cell–specific ablation of mTOR severely decreased T_{FH} and GC B cell formation in mLNs and PP, sites where spontaneous accumulation of T_{FH} cells occur in LDS mice. We found that elevated transcription of *Pik3cg* is likely an important factor driving enhanced PI3K/mTOR signaling in LDS. *Pik3cg* encodes the protein p110γ, which associates with p85 to form the PI3K class IB molecule PI3Kγ. PI3Kγ is highly expressed in leukocytes and is activated downstream of TCR signaling (*59*). PI3Kγ-deficient mice have been reported to exhibit impaired phosphorylation of AKT and S6 and defective T cell–mediated humoral responses (*57*, *58*). Similarly, patients with biallelic loss-of-function *PIK3CG* variants exhibit immunodeficiency and decreased antibody levels (*56*, *57*). These reports highlight a critical role for PI3Kγ in T cell function and humoral immunity. Here, we identify TGFβ to be a critical regulator of PI3Kγ activity. Treatment with a PI3Kγ-specific inhibitor was able to reduce elevated levels of late-phase TCR-induced pS6 and pFOXO1 in LDS patient T cells to levels found in HV T cells. Furthermore, in vivo PI3Kγ or mTOR inhibition restrained differentiation of $T_{FH}2$ cells and antigen-specific IgE and IgG1 production in *Tgfbr1*$^{WT/mut}$ mice after oral feeding. Collectively, these studies reveal a key role for *Pik3cg* in driving the allergic phenotype in LDS and further indicate a role for *Pik3cg* in allergic diseases in general.

The mechanisms by which TGFβ regulates *Pik3cg* expression are likely multifactorial, but our data support a role for the transcriptional repressor *Skil*/SnoN. Expression of *Skil*/SnoN was reduced in *Tgfbr1*$^{WT/mut}$ T_{FH} cells directly ex vivo, and induction of *Skil*/SnoN was impaired in PP naïve $CD4^+$ *Tgfbr1*$^{WT/mut}$ T cells relative to WT in the late phase after TCR activation. Similarly, levels of pS6 and pFoxO1 were equal in *Tgfbr1*$^{WT/mut}$ and WT PP naïve $CD4^+$ T cells early after TCR stimulation but increased in the late phase, indicating that the changes in expression of *Skil*/SnoN and signaling molecules downstream of PI3Kγ in LDS T cells were temporally correlated. In combination with our findings that KD of *Skil*/SnoN abrogates pS6 expression in WT naïve $CD4^+$ T cells after TCR cross-linking, our data point to reduced *Skil*/SnoN as a potential mechanism by which impaired canonical TGFβ signaling results in enhanced PI3K activity. Although other mechanisms may contribute, mixing experiments indicated that soluble factors were unlikely to play a prominent role. How these changes in the late phase of TCR signaling contribute to the differential regulation of T_{FH} subtypes requires further study.

One limitation of our study is the inability to differentiate $T_{FH}2$ cells in vitro, which limits more in-depth mechanistic examination of the role of *Skil*/SnoN and PI3Kγ in $T_{FH}2$ cell differentiation. Additional investigation is warranted to further dissect the role of this critical pathway in T_{FH} development. Although our data point to impaired canonical TGFβ signaling as the key driver of the defects in T_{FH} development in LDS, our data do not preclude a role for noncanonical TGFβ signaling in the allergic phenotype as well. Last, although our data demonstrate a T cell–intrinsic phenotype, the contribution of other cell types in the hyper-IgE phenotype in LDS warrants further study.

In summary, our work supports a nonredundant T cell–intrinsic role for TGFβ in restricting spontaneous $T_{FH}2$ cell differentiation in response to innocuous antigens that is conserved across species. Impairment of TGFβ signaling leads to exaggerated humoral immunity that manifests clinically as IgE-mediated disease, thus providing insight into the role of TGFβ in the pathogenesis of allergic disorders. Future studies will examine the mechanisms by which SnoN and PI3Kγ regulate $T_{FH}2$ differentation and the implications for allergic diseases.

MATERIALS AND METHODS

Study design

Patients with LDS exhibit a high prevalence of allergic diseases. Samples from patients with LDS and a mouse model of LDS, *Tgfbr1*$^{WT/mut}$, were used to interrogate the mechanistic role of TGFβ signaling in regulating IgE production and allergic sensitization to antigens. Age- and sex-matched HVs and WT littermates were used as controls. We characterized serum Ig profiles and immune cell populations from peripheral blood of humans and lymphoid organs in mice. Further in vitro differentiation and TCR stimulations were performed on purified naïve human T cells, followed by supernatant enzyme-linked immunosorbent assay (ELISA), qPCR, and flow cytometry analysis. An adoptive transfer oral tolerance model and BM and FL chimeras were used along with ELISAs, flow cytometry, bulk RNA-seq, and scRNA-seq analysis to assess the cellular and signaling pathways involved.

Mice

The mouse model of LDS is described in Gallo *et al.* (*36*). Briefly, the *M318R* allele previously identified in patients with LDS was knocked into the mouse *Tgfbr1* locus, resulting in heterozygous *Tgfbr1*$^{WT/mut}$ mice. The immune phenotype of LDS mice is further characterized in Laky *et al.* (*40*). This colony was bred and maintained at Taconic Farms and shipped to National Institute of Allergy and Infectious Diseases (NIAID) weekly per the NIAID-Taconic Breeding contract.

OTII mice, CD45.1, and RAG2$^{-/-}$ mice were also from Taconic, and IgE knockout mice were provided by H. Oettgen (*71*). All mice were backcrossed to 129/SVe for at least 12 generations, and WT littermates served as controls for all experiments. All murine experiments were done following National Institutes of Health (NIH) Association for Assessment and Accreditation of Laboratory Animal Care regulations and were approved by the NIAID Animal Care and Use Committee. Unless otherwise stated, mice were provided with standard mouse chow and autoclaved water. Some mice were fed a wheat-free diet (DietGel 31M) from birth as a negative control for wheat IgE production in mice fed standard mouse chow. WT and *Tgfbr1*$^{WT/mut}$ mice, including the mice used in reconstitution and adoptive transfer experiments, were cohoused. Both sexes of mice between the ages of 22 and 36 weeks old were used in this study.

Human samples

Patients with a diagnosis of type 1 (mutations in *TGFBR1*) or 2 (mutations in *TGFBR2*) LDS confirmed by genetic testing, patients with nonsyndromic IgE-mediated food allergy, and healthy controls were enrolled on clinical protocol 15-I-0152 at the NIH. Food allergic patients were diagnosed by a board-certified allergist on the basis of a convincing history of an immediate hypersensitivity reaction to the food and positive food-specific IgE testing. Patients underwent a full clinical allergy evaluation as well as blood work, including measurement of serum Igs and allergen-specific IgE for common food and environmental allergens (Phadia, ImmunoCAP). Allergen-specific IgE levels greater than 0.35 KU_A/liter were reported as positive. This study was approved by the NIH institutional review board, and informed consent and/or assent were obtained.

HV and LDS PBMCs were isolated by Percoll gradient centrifugation and stained for flow cytometry on the same day. Cells were stained with Zombie Aqua live dead dye (BioLegend) and then washed and blocked with human Ig after staining with the T_{FH} cell panel or the B cell panel (table S2). After surface staining, cells were fixed with Foxp3 transcription factor staining fixation buffer (Thermo Fisher Scientific) and stained for Foxp3. Cells were then analyzed by flow cytometry (BD LSRII), or $T_{FH}1$, $T_{FH}2$, and $T_{FH}17$ cells were sorted (BD FACS Aria), rested overnight, stimulated with PMA/ionomycin/brefeldin A cocktail (Invitrogen) for 4 hours, and then stained intracellularly for anti–IFN-γ, anti–IL-4, anti–IL-13, anti–IL-17, and anti–IL-21. Live, singlet, $CD4^+$, and $CD8^-$ cells were gated. T_{FH} cells were then identified as $CD45RO^+CXCR5^+$. Within this gate, $T_{FH}1$ cells were defined as $CXCR3^+CCR6^-$, $T_{FH}2$ as $CCR4^+CCR6^-$, $T_{FH}17$ as $CCR6^+CXCR3^-$, and Tfr as $CXCR5^+CD45RO^+CD25^+Foxp3^+$. Naïve B cells were defined as live, singlet, $CD19^+CD3^-CD20^+CD27^-CD10^-CD21^+IgM^+IgD^+$. Plasmablasts were defined as live, singlet, $CD19^+CD3^-CD20^+CD27^+CD10^-CD38$med/high.

Mixing and chimeric transfer models

For mixed chimeras, BM was harvested from femurs of IgE$^{-/-}$ CD45.2 age- and sex-matched mice and mixed in equal parts (2.5 million cells each) with embryonic 12-day CD45.1 WT or *Tgfbr1*$^{WT/mut}$ FL cells. Fetal liver lacks mature plasma cells, which are abundant in the BM of adult animals; thus, in this model, all IgE-producing plasma cells matured in the host. This ensured that the only source of serum IgE was de novo plasma cells that matured in the recipient host. The mixed cells were administered intravenously into sublethally irradiated (600 RADS) RAG$^{-/-}$ age- and sex-matched hosts. Serum was collected at 8 weeks posttransfer, and total IgE was measured using an ELISA kit (BioLegend). For BM chimera experiments, BM was harvested from CD45.1 WT mice and CD45.2 *Tgfbr1*$^{WT/mut}$ mice, mixed in equal parts, and transferred into sublethally irradiated RAG$^{-/-}$ mice. PP and mLNs were collected at 4 months posttransfer, mashed through 70-μm filters to make single-cell suspensions, and analyzed by flow cytometry using the T_{FH} staining panel described above.

OVA in FCA immunization

Phosphate-buffered saline (PBS) to FCA (1:1; Sigma-Aldrich) were emulsified for a final concentration of 250 μg/ml, and 20 μl was injected into the left footpads of WT or *Tgfbr1*$^{WT/mut}$ mice. Serum was collected on days 0, 14, and 21 to measure antigen-specific Ig. Nondraining and draining popliteal lymph nodes were collected at day 21, and cells were analyzed by flow cytometry.

PP histology

For immunofluorescence staining, PP were fixed overnight in BD CytoFix fixation buffer diluted 1:4 in PBS. Tissues were then rinsed with PBS and moved to 30% sucrose in PBS overnight. Tissue was embedded in optimal cutting temperature compound (OTC) (Sakura) and frozen in a mixture of isopentane and dry ice and sectioned at 10 μm (Histoserv). The slides were permeabilized in methanol at −20°C for 30 min, washed in PBS, and then blocked with 1% bovine serum albumin,1% anti-CD16/32 (BD), 2% mouse serum, 2% goat serum, 2% rat serum, and 0.3% Triton X-100 in PBS for 1 hour at room temperature. The slides were then stained with anti-B220, anti-IgD, anti-Bcl6, and anti-CD4 at 4°C overnight. The next day, the slides were stained with 4′,6-diamidino-2-phenylindole at 1 μg/ml for 10 min at room temperature, washed in PBS, and mounted in ProLong Gold Antifade Mountant (Thermo Fisher Scientific). Images were obtained on a Leica SP8 confocal microscope and analyzed using LAS X imaging software.

In vitro T cell assays

For in vitro suppression studies, naïve $CD4^+$ T cells were sorted and labeled with CellTrace Violet (Invitrogen) and then cultured in vitro with indicated ratios of $CD4^+CD25^+$ T_{regs} for 5 days. Proliferation was measured by flow cytometry. Percent suppression was determined using the division index (DI) obtained from FlowJo and the calculation (DI without T_{reg} − DI with T_{regs})/(DI without T_{regs}) × 100.

For in vitro pS6 and pFoxO1 analysis, naïve $CD4^+$ T cells from murine PP ($CD4^+CD8^-CD62L^+$) or human peripheral blood ($CD45RO^-CD4^+CD8^-CD19^-CXCR5^-$) were sorted then stimulated with plate-bound anti-CD3 (1 μg/ml; human: BioLegend: clone OKT3; mouse: Invitrogen: clone 145-2C11) and soluble anti-CD28 (5 μg/ml; human: Invitrogen, clone CD28.2, mouse: BioLegend: clone 37.51) for indicated time points for murine cells and 68 hours for human cells. In some experiments, CD45.1 and CD45.2 murine PP naïve T cells were mixed and stimulated in the same well. The frequencies of IL-2–secreting cells at 16 hours after anti-CD3/CD28 stimulation were measured using the IL-2 secretion assay detection kit (Miltenyi) following the manufacturer's protocol. In some experiments, human T cells were treated with 0.5 μM eganelisib or vehicle (dimethyl sulfoxide) for 1 hour before anti-CD3/CD28 stimulation. In some experiments, murine T cells were treated with an IgG1 isotype (R&D MAB002) or anti-TGFβ (R&D MAB1835-100) at 10 or 20 μg/ml at the time of anti-CD3/CD28 stimulation. In Fig. 6K, fold induction was determined by dividing the % + pS6 in stimulated sample by its corresponding unstimuated control.

For siRNA KD assays, naïve WT spleens were harvested, T cells were purified using the negative selection T cell isolation kit (Miltenyi Biotech) and transfected using scramble control or a pool of four different *Skil*/SnoN-specific siRNA (Qiagen) on the Nucleofector 2b Device (Lonza) using the murine T cell kit (Lonza) following manufacturer's instructions. Twenty-four hours after transfection, cells were washed and stimulated by plate-bound anti-CD3 and soluble anti-CD28 as described above. Cells were then fixed in 2% paraformaldehyde for 10 min, washed twice in PBS, and permeabilized in ice-cold methanol overnight at 4°C or 1 hour at −20° C. Cells were stained with anti-pS6 and anti-SnoN and conjugated with an Alexa Fluor 647 labeling kit following the manufacturer's instructions (Thermo Fisher Scientific) for 1 hour at 4°C and analyzed by flow cytometry. Fold induction was calculated by dividing the activated sample by its unactivated control.

For pSmad2/3 detection, mouse splenocytes and thawed cryopreserved human PBMCs were serum-starved overnight in 0.1% serum in complete Iscove's modified Dulbecco's medium (cIMDM) for murine cells (0.1% penicillin/streptomycin, 50 μM Gibco 2-mercaptoethanol) and serum-free AIM-V media for human cells. The next day, cells were stimulated with recombinant human TGFβ (0.5 ng/ml; R&D) for the indicated time point. Cells were fixed using the BD phosphoflow kit following the manufacturer's instructions. Cells were stained with anti-CD4, anti-TCRβ, anti-CD25, anti-CD45RO, and anti-pSMAD2/3 at 4°C for 1 hour and analyzed by flow cytometry.

For human T_{FH} differentiation, sorted naïve T cells from PBMCs were stained for CellTrace Violet and then plated in AIM-V media (Gibco) at 500,000 cells/ml with recombinant human IL-7 (PeproTech) at 4 ng/ml, with or without recombinant IL-12 (PeproTech) at 5 ng/ml, and recombinant TGFβ (R&D) at 1 ng/ml for 5 days. Cells were added to plates coated with anti-CD4 and anti–inducible costimulator ligand (ICOSL) (BioLegend) at 5 mg/ml. On day 5, cells were collected, and flow cytometry was used to determine CXCR5 expression or stored in TRIzol for qPCR analysis.

Bulk RNA-seq analysis and statistics

PP $CD4^+CXCR5^+PD^-1^+$ T_{FH} cells were sorted on a BD FACS Aria and stored in TRIzol. Total RNA was collected using the chloroform and ethanol isolation method. Clontech SMART-Seq Ultra Low Input Non-Stranded mRNA Library Prep was used on a total of 300 pg of RNA according to the manufacturer's protocol. The final purified product was then quantitated by qPCR before cluster generation and sequencing on the NextSeq sequencer. Raw fastq files were then trimmed for quality and adapter contamination using Cutadapt v2.10, and trimmed reads were mapped to the murine reference genome and Ensembl v103 transcriptome using STAR v2.5.3 in two-pass mode (*72*, *73*). Gene-level expression quantification was performed using RSEM v1.3.0, and standard differential expression was performed using the R package DESeq2 as implemented in iDEP 0.92 (*74*–*76*). Before differential expression and downstream time course analysis, genes were filtered that had <1 counts per million across >3 samples. For pathway analysis, we used two approaches. First, we conducted GSEA (*77*, *78*) using three gene sets created using data from publicly available data (*54*, *55*, *79*). The gene set used in the "TGFβ/Smad3-induced Genes" analysis was obtained from a published source (GSE40494) (*54*). The "Raptor- and Rictor-Dependent Genes" and "Gene-Enriched in T_{FH} cells versus non-T_{FH}" gene sets were created using Partek Genomics Suite to call differentially expressed genes by analysis of variance (ANOVA) [GSE85555, GSE21380; false discovery rate (FDR) < 0.1] (*55*, *79*). In addition to GSEA, we performed pathway enrichment using the top 500 differentially expressed genes based on FDR less than 0.1 as input to the core analysis of Qiagen's IPA platform. Raw data have been deposited into Gene Expression Omnibus (GEO) under the accession number GSE203379.

Statistical analysis

One-way ANOVA analyses were performed for experiments involving more than one group with one variable. Two-way ANOVA was used for experiments involving more than one groups, with two variables. Two-tailed paired Student's *t* test was used to analyze 50:50 BM chimera and siRNA KD data. For comparing two unpaired groups, Mann-Whitney nonparametric tests were used. All analyses other than RNA-seq analysis were done using GraphPad Prism. All replicates are biological replicates, and *n* values are listed for each group. Additional materials and methods can be found in the Supplementary Materials.

Supplementary Materials

This PDF file includes:
Figs. S1 to S10
Tables S1 to S3
References (*80*–*82*)

Other Supplementary Material for this manuscript includes the following:
Data files S1 to S5
MDAR Reproducibility Checklist

REFERENCES AND NOTES

1. B. J. H. Dierick, T. van der Molen, B. M. J. Flokstra-de Blok, A. Muraro, M. J. Postma, J. W. H. Kocks, J. F. M. van Boven, Burden and socioeconomics of asthma, allergic rhinitis, atopic dermatitis and food allergy. *Expert Rev. Pharmacoecon. Outcomes Res.* **20**, 437–453 (2020).
2. T. A. Olafsdottir, F. Theodors, K. Bjarnadottir, U. S. Bjornsdottir, A. B. Agustsdottir, O. A. Stefansson, E. V. Ivarsdottir, J. K. Sigurdsson, S. Benonisdottir, G. I. Eyjolfsson, D. Gislason, T. Gislason, S. Guðmundsdóttir, A. Gylfason, B. V. Halldorsson, G. H. Halldorsson, T. Juliusdottir, A. M. Kristinsdottir, D. Ludviksdottir, B. R. Ludviksson, G. Masson, K. Norland, P. T. Onundarson, I. Olafsson, O. Sigurdardottir, L. Stefansdottir, G. Sveinbjornsson, V. Tragante, D. F. Gudbjartsson, G. Thorleifsson, P. Sulem, U. Thorsteinsdottir, G. L. Norddahl, I. Jonsdottir, K. Stefansson, Eighty-eight variants highlight the role of T cell regulation and airway remodeling in asthma pathogenesis. *Nat. Commun.* **11**, 393 (2020).
3. K. Hatsushika, T. Hirota, M. Harada, M. Sakashita, M. Kanzaki, S. Takano, S. Doi, K. Fujita, T. Enomoto, M. Ebisawa, S. Yoshihara, H. Sagara, K. Fukuda, K. Masuyama, R. Katoh, K. Matsumoto, H. Saito, H. Ogawa, M. Tamari, A. Nakao, Transforming growth factor-β_2 polymorphisms are associated with childhood atopic asthma. *Clin. Exp. Allergy* **37**, 1165–1174 (2007).
4. M. A. Portelli, E. Hodge, I. Sayers, Genetic risk factors for the development of allergic disease identified by genome-wide association. *Clin. Exp. Allergy* **45**, 21–31 (2015).
5. J. K. Pickrell, T. Berisa, J. Z. Liu, L. Ségurel, J. Y. Tung, D. A. Hinds, Detection and interpretation of shared genetic influences on 42 human traits. *Nat. Genet.* **48**, 709–717 (2016).
6. K. Valette, Z. Li, V. Bon-Baret, A. Chignon, J. C. Bérubé, A. Eslami, J. Lamothe, N. Gaudreault, P. Joubert, M. Obeidat, M. van den Berge, W. Timens, D. D. Sin, D. C. Nickle, K. Hao, C. Labbé, K. Godbout, A. Côté, M. Laviolette, L. P. Boulet, P. Mathieu, S. Thériault, Y. Bossé, Prioritization of candidate causal genes for asthma in susceptibility loci derived from UK Biobank. *Commun. Biol.* **4**, 700 (2021).
7. Y. Han, Q. Jia, P. S. Jahani, B. P. Hurrell, C. Pan, P. Huang, J. Gukasyan, N. C. Woodward, E. Eskin, F. D. Gilliland, O. Akbari, J. A. Hartiala, H. Allayee, Genome-wide analysis highlights contribution of immune system pathways to the genetic architecture of asthma. *Nat. Commun.* **11**, 1776 (2020).
8. G. Kichaev, G. Bhatia, P. R. Loh, S. Gazal, K. Burch, M. K. Freund, A. Schoech, B. Pasaniuc, A. L. Price, Leveraging polygenic functional enrichment to improve GWAS power. *Am. J. Hum. Genet.* **104**, 65–75 (2019).
9. P. D. Arkwright, T. J. David, J. M. Chase, S. Babbage, V. Pravica, I. V. Hutchinson, Atopic dermatitis is associated with a low-producer transforming growth factor β_1 cytokine genotype. *J. Allergy Clin. Immunol.* **108**, 281–284 (2001).

10. K. Hobbs, J. Negri, M. Klinnert, L. J. Rosenwasser, L. Borish, Interleukin-10 and transforming growth factor- β promoter polymorphisms in allergies and asthma. *Am. J. Respir. Crit. Care Med.* **158**, 1958–1962 (1998).
11. V. Verhasselt, V. Milcent, J. Cazareth, A. Kanda, S. Fleury, D. Dombrowicz, N. Glaichenhaus, V. Julia, Breast milk-mediated transfer of an antigen induces tolerance and protection from allergic asthma. *Nat. Med.* **14**, 170–175 (2008).
12. M. A. Pérez-Machado, P. Ashwood, M. A. Thomson, F. Latcham, R. Sim, J. A. Walker-Smith, S. H. Murch, Reduced transforming growth factor-β1-producing T cells in the duodenal mucosa of children with food allergy. *Eur. J. Immunol.* **33**, 2307–2315 (2003).
13. W. H. Oddy, M. Halonen, F. D. Martinez, I. C. Lohman, D. A. Stern, M. Kurzius-Spencer, S. Guerra, A. L. Wright, TGF-β in human milk is associated with wheeze in infancy. *J. Allergy Clin. Immunol.* **112**, 723–728 (2003).
14. W. Scherf, S. Burdach, G. Hansen, Reduced expression of transforming growth factor β_1 exacerbates pathology in an experimental asthma model. *Eur. J. Immunol.* **35**, 198–206 (2005).
15. K. Nagpal, S. Sharma, C. B-Rao, S. Nahid, P. V. Niphadkar, S. K. Sharma, B. Ghosh, *TGFβ1* haplotypes and asthma in Indian populations. *J. Allergy Clin. Immunol.* **115**, 527–533 (2005).
16. T. Ando, K. Hatsushika, M. Wako, T. Ohba, K. Koyama, Y. Ohnuma, R. Katoh, H. Ogawa, K. Okumura, J. Luo, T. Wyss-Coray, A. Nakao, Orally administered TGF-β is biologically active in the intestinal mucosa and enhances oral tolerance. *J. Allergy Clin. Immunol.* **120**, 916–923 (2007).
17. A. Okamoto, T. Kawamura, K. Kanbe, Y. Kanamaru, H. Ogawa, K. Okumura, A. Nakao, Suppression of serum IgE response and systemic anaphylaxis in a food allergy model by orally administered high-dose TGF-β. *Int. Immunol.* **17**, 705–712 (2005).
18. S. Holvoet, M. Perrot, N. de Groot, G. Prioult, T. Mikogami, V. Verhasselt, S. Nutten, Oral tolerance induction to newly introduced allergen is favored by a transforming growth Factor-β-Enriched formula. *Nutrients* **11**, 2210 (2019).
19. H. Loeys, H. C. Dietz, Loeys-Dietz Syndrome. *GeneReviews* **55–61**, (2017).
20. P. A. Frischmeyer-Guerrerio, A. L. Guerrerio, G. Oswald, K. Chichester, L. Myers, M. K. Halushka, M. Oliva-Hemker, R. A. Wood, H. C. Dietz, Allergy: TGFβ receptor mutations impose a strong predisposition for human allergic disease. *Sci. Transl. Med.* **5**, 195ra94 (2013).
21. C. G. Vinuesa, M. A. Linterman, D. Yu, I. C. M. Maclennan, Follicular Helper T Cells. *Annu. Rev. Immunol.* **34**, 335–368 (2016).
22. S. Crotty, T follicular helper cell biology: A decade of discovery and diseases. *Immunity* **50**, 1132–1148 (2019).
23. C. H. Kim, L. S. Rott, I. Clark-Lewis, D. J. Campbell, L. Wu, E. C. Butcher, Subspecialization of $CXCR5^+$ T cells: B helper activity is focused in a germinal center-localized subset of $CXCR5^+$ T cells. *J. Exp. Med.* **193**, 1373–1382 (2001).
24. Y. Che, J. Qiu, T. Jin, F. Yin, M. Li, Y. Jiang, Circulating memory T follicular helper subsets, Tfh2 and Tfh17, participate in the pathogenesis of Guillain-Barré syndrome. *Sci. Rep.* **6**, 20963 (2016).
25. R. Morita, N. Schmitt, S. E. Bentebibel, R. Ranganathan, L. Bourdery, G. Zurawski, E. Foucat, M. Dullaers, S. Oh, N. Sabzghabaei, E. M. Lavecchio, M. Punaro, V. Pascual, J. Banchereau, H. Ueno, Human blood $CXCR5^+CD4^+$ T cells are counterparts of T follicular cells and contain specific subsets that differentially support antibody secretion. *Immunity* **34**, 108–121 (2011).
26. U. Gowthaman, J. S. Chen, B. Zhang, W. F. Flynn, Y. Lu, W. Song, J. Joseph, J. A. Gertie, L. Xu, M. A. Collet, J. D. S. Grassmann, T. Simoneau, D. Chiang, M. Cecilia Berin, J. E. Craft, J. S. Weinstein, A. Williams, S. C. Eisenbarth, Identification of a T follicular helper cell subset that drives anaphylactic IgE. *Science* **365**, eaaw6433 (2019).
27. A. Noble, J. Zhao, Follicular helper T cells are responsible for IgE responses to Der p 1 following house dust mite sensitization in mice. *Clin. Exp. Allergy* **46**, 1075–1082 (2016).
28. A. P. Meli, G. Fontes, C. L. Soo, I. L. King, T follicular helper cell-derived IL-4 is required for IgE production during intestinal helminth infection. *J. Immunol.* **199**, 244–252 (2017).
29. I. L. King, M. Mohrs, IL-4-producing $CD4^+$ T cells in reactive lymph nodes during helminth infection are T follicular helper cells. *J. Exp. Med.* **206**, 1001–1007 (2009).
30. F. Gong, H. Y. Zhu, J. Zhu, Q. J. Dong, X. Huang, D. J. Jiang, Circulating $CXCR5^+$ $CD4^+$ T cells participate in the IgE accumulation in allergic asthma. *Immunol. Lett.* **197**, 9–14 (2018).
31. Y. Yao, C. L. Chen, N. Wang, Z. C. Wang, J. Ma, R. F. Zhu, X. Y. Xu, P. C. Zhou, D. Yu, Z. Liu, Correlation of allergen-specific T follicular helper cell counts with specific IgE levels and efficacy of allergen immunotherapy. *J. Allergy Clin. Immunol.* **142**, 321–324.e10 (2018).
32. H. D. Marshall, J. P. Ray, B. J. Laidlaw, N. Zhang, D. Gawande, M. M. Staron, J. Craft, S. M. Kaech, The transforming growth factor beta signaling pathway is critical for the formation of CD4 T follicular helper cells and isotype-switched antibody responses in the lung mucosa. *eLife* **4**, e04851 (2015).
33. M. J. McCarron, J. C. Marie, TGF-β prevents T follicular helper cell accumulation and B cell autoreactivity. *J. Clin. Invest.* **124**, 4375–4386 (2014).
34. M. Locci, J. E. Wu, F. Arumemi, Z. Mikulski, C. Dahlberg, A. T. Miller, S. Crotty, Activin A programs the differentiation of human TFH cells. *Nat. Immunol.* **17**, 976–984 (2016).
35. N. Schmitt, Y. Liu, S.-E. Bentebibel, I. Munagala, L. Bourdery, K. Venuprasad, J. Banchereau, H. Ueno, The cytokine TGF-β co-opts signaling via STAT3-STAT4 to promote the differentiation of human TFH cells. *Nat. Immunol.* **15**, 856–865 (2014).
36. E. M. Gallo, D. C. Loch, J. P. Habashi, J. F. Calderon, Y. Chen, D. Bedja, C. Van Erp, E. E. Gerber, S. J. Parker, K. Sauls, D. P. Judge, S. K. Cooke, M. E. Lindsay, R. Rouf, L. Myers, M. Colette, K. C. Kent, R. A. Norris, D. L. Huso, H. C. Dietz, Angiotensin II–dependent TGF-β signaling contributes to Loeys-Dietz syndrome vascular pathogenesis. *J. Clin. Invest.* **124**, 448–460 (2014).
37. S. Cardoso, S. P. Robertson, P. B. Daniel, TGFBR1 mutations associated with Loeys-Dietz syndrome are inactivating. *J. Recept. Signal Transduct.Res.* **32**, 150–155 (2012).
38. T. Mizuguchi, G. Collod-Beroud, T. Akiyama, M. Abifadel, N. Harada, T. Morisaki, D. Allard, M. Varret, M. Claustres, H. Morisaki, M. Ihara, A. Kinoshita, K.-I. Yoshiura, C. Junien, T. Kajii, G. Jondeau, T. Ohta, T. Kishino, Y. Furukawa, Y. Nakamura, N. Niikawa, C. Boileau, N. Matsumoto, G. Jondeau, T. Ohta, Heterozygous *TGFBR2* mutations in Marfan syndrome. *Nat. Genet.* **36**, 855–860 (2004).
39. M. O. Li, S. Sanjabi, R. A. A. Flavell, Transforming growth factor-β controls development, homeostasis, and tolerance of T cells by regulatory T cell-dependent and -independent mechanisms. *Immunity* **25**, 455–471 (2006).
40. K. Laky, J. L. Kinard, J. M. Li, I. N. Moore, J. Lack, E. R. Fischer, J. Kabat, R. Latanich, N. C. Zachos, A. R. Limkar, K. A. Weissler, R. W. Thompson, T. A. Wynn, H. C. Dietz, A. L. Guerrerio, P. A. Frischmeyer-Guerrerio, Epithelial-intrinsic defects in TGFβR signaling drive local allergic inflammation manifesting as eosinophilic esophagitis. *Sci. Immunol.* **8**, eabp9940 (2023).
41. A. P. Mountford, A. Fisher, R. A. Wilson, The profile of IgG1 and IgG2a antibody responses in mice exposed to Schistosoma mansoni. *Parasite Immunol.* **16**, 521–527 (1994).
42. F. Teng, C. N. Klinger, K. M. Felix, C. P. Bradley, E. Wu, N. L. Tran, Y. Umesaki, H. J. J. Wu, Gut microbiota drive autoimmune arthritis by promoting differentiation and migration of Peyer's Patch T follicular helper cells. *Immunity* **44**, 875–888 (2016).
43. Y. Zhang, P. B. Alexander, X. F. Wang, TGF-β family signaling in the control of cell proliferation and survival. *Cold Spring Harb. Perspect. Biol.* **9**, a022145 (2017).
44. C. A. Akdis, M. Akdis, Mechanisms and treatment of allergic disease in the big picture of regulatory T cells. *J. Allergy Clin. Immunol.* **123**, 735–746 (2009).
45. J. M. Moreau, M. Velegraki, C. Bolyard, M. D. Rosenblum, Z. Li, Transforming growth factor-β1 in regulatory T cell biology. *Sci. Immunol.* **7**, eabi4613 (2022).
46. J. M. Moreau, M. O. Dhariwala, V. Gouirand, D. P. Boda, I. C. Boothby, M. M. Lowe, J. N. Cohen, C. E. Macon, J. M. Leech, L. A. Kalekar, T. C. Scharschmidt, M. D. Rosenblum, Regulatory T cells promote innate inflammation after skin barrier breach via TGF-β activation. *Sci. Immunol.* **6**, eabg2329 (2021).
47. S. Budhu, D. A. Schaer, Y. Li, R. Toledo-Crow, K. Panageas, X. Yang, H. Zhong, A. N. Houghton, S. C. Silverstein, T. Merghoub, J. D. Wolchok, Blockade of surface-bound TGF-β on regulatory T cells abrogates suppression of effector T cell function in the tumor microenvironment. *Sci. Signal.* **10**, (2017).
48. E. C. Steinbach, G. R. Gipson, S. Z. Sheikh, Induction of murine intestinal inflammation by adoptive transfer of effector $CD4^+CD45RB^{high}$ T cells into immunodeficient mice. *J. Vis. Exp.* **2015**, 52533 (2015).
49. M. Kamanaka, S. Huber, L. A. Zenewicz, N. Gagliani, C. Rathinam, W. O'Connor Jr., Y. Y. Wan, S. Nakae, Y. Iwakura, L. Hao, R. A. Flavell, Memory/effector ($CD45RB^{lo}$) CD4 T cells are controlled directly by IL-10 and cause IL-22–dependent intestinal pathology. *J. Exp. Med.* **208**, 1027–1040 (2011).
50. B. Miles, S. M. Miller, J. M. Folkvord, A. Kimball, M. Chamanian, A. L. Meditz, T. Arends, M. D. McCarter, D. N. Levy, E. G. Rakasz, P. J. Skinner, E. Connick, Follicular regulatory T cells impair follicular T helper cells in HIV and SIV infection. *Nat. Commun.* **6**, 8608 (2015).
51. M. A. Linterman, W. Pierson, S. K. Lee, A. Kallies, S. Kawamoto, T. F. Rayner, M. Srivastava, D. P. Divekar, L. Beaton, J. J. Hogan, S. Fagarasan, A. Liston, K. G. C. Smith, C. G. Vinuesa, $Foxp3^+$ follicular regulatory T cells control the germinal center response. *Nat. Med.* **17**, 975–982 (2011).
52. T. C. Moore, R. J. Messer, K. J. Hasenkrug, Regulatory T cells suppress virus-specific antibody responses to Friend retrovirus infection. *PLOS ONE* **13**, e0195402 (2018).
53. H. W. Lim, P. Hillsamer, A. H. Banham, C. H. Kim, Cutting edge: Direct suppression of B cells by $CD4^+CD25^+$ regulatory T cells. *J. Immunol.* **175**, 4180–4183 (2005).
54. J.-S. Delisle, M. Giroux, G. Boucher, J.-R. Landry, M.-P. Hardy, S. Lemieux, R. G. Jones, B. T. Wilhelm, C. Perreault, The TGF-β-Smad3 pathway inhibits CD28-dependent cell growth and proliferation of CD4 T cells. *Genes Immun.* **14**, 115–126 (2013).
55. I. Yusuf, R. Kageyama, L. Monticelli, R. J. Johnston, D. DiToro, K. Hansen, B. Barnett, S. Crotty, Germinal center T follicular helper cell IL-4 production is dependent on signaling lymphocytic activation molecule receptor (CD150). *J. Immunol.* **185**, 190–202 (2010).
56. M. Thian, B. Hoeger, A. Kamnev, F. Poyer, S. K. Bal, M. Caldera, R. Jiménez-Heredia, J. Huemer, W. F. Pickl, M. Groß, S. Ehl, C. L. Lucas, J. Menche, C. Hutter, A. Attarbaschi, L. Dupré, K. Boztug, Germline biallelic PIK3CG mutations in a multifaceted immunodeficiency with immune dysregulation. *Haematologica* **105**, e488 (2020).
57. A. J. Takeda, T. J. Maher, Y. Zhang, S. M. Lanahan, M. L. Bucklin, S. R. Compton, P. M. Tyler, W. A. Comrie, M. Matsuda, K. N. Olivier, S. Pittaluga, J. J. McElwee, D. A. Long Priel,

D. B. Kuhns, R. L. Williams, P. J. Mustillo, M. P. Wymann, V. Koneti Rao, C. L. Lucas, Human PI3Kγ deficiency and its microbiota-dependent mouse model reveal immunodeficiency and tissue immunopathology. *Nat. Commun.* **10**, 4364 (2019).
58. T. Sasaki, J. Irie-Sasaki, R. G. Jones, A. J. Oliveira-Dos-Santos, W. L. Stanford, B. Bolon, A. Wakeham, A. Itie, D. Bouchard, I. Kozieradzki, N. Joza, T. W. Mak, P. S. Ohashi, A. Suzuki, J. M. Penninger, Function of PI3Kγ in thymocyte development, T cell activation, and neutrophil migration. *Science* **287**, 1040–1046 (2000).
59. I. Alcázar, M. Marqués, A. Kumar, E. Hirsch, M. Wymann, A. C. Carrera, D. F. Barber, Phosphoinositide 3-kinase gamma participates in T cell receptor-induced T cell activation. *J. Exp. Med.* **204**, 2977–2987 (2007).
60. A. C. Tecalco-Cruz, M. Sosa-Garrocho, G. Vázquez-Victorio, L. Ortiz-García, E. Domínguez-Hüttinger, M. Macías-Silva, Transforming growth factor-β/SMAD Target gene SKIL is negatively regulated by the transcriptional cofactor complex SNON-SMAD4. *J. Biol. Chem.* **287**, 26764–26776 (2012).
61. Q. Zhu, S. Pearson-White, K. Luo, Requirement for the SnoN oncoprotein in transforming growth factor β-induced oncogenic transformation of fibroblast cells. *Mol. Cell. Biol.* **25**, 10731–10744 (2005).
62. S. L. Stroschein, W. Wang, S. Zhou, Q. Zhou, K. Luo, Negative feedback regulation of TGF-β signaling by the SnoN oncoprotein. *Science* **286**, 771–774 (1999).
63. A. Ballesteros-Tato, B. León, B. A. Graf, A. Moquin, P. S. Adams, F. E. Lund, T. D. Randall, Interleukin-2 inhibits germinal center formation by limiting T follicular helper cell differentiation. *Immunity* **36**, 847–856 (2012).
64. S. Korten, A. Hoerauf, J. T. Kaifi, D. W. Büttner, Low levels of transforming growth factor-beta (TGF-beta) and reduced suppression of Th2-mediated inflammation in hyperreactive human onchocerciasis. *Parasitology* **138**, 35–45 (2011).
65. G. Ciprandi, M. De Amici, M. A. Tosca, A. Pistorio, G. L. Marseglia, Sublingual immunotherapy affects specific antibody and TGF-beta serum levels in patients with allergic rhinitis. *Int. J. Immunopathol. Pharmacol.* **22**, 1089–1096 (2009).
66. T. Kobayashi, K. Iijima, C.-C. Chen, A. L. Dent, H. Kita, Follicular helper T (Tfh) cells are indispensable for IgE antibody responses to airborne allergens. *J. Allergy Clin. Immunol.* **137**, AB1 (2016).
67. J. J. Dolence, T. Kobayashi, K. Iijima, J. Krempski, L. Y. Drake, A. L. Denty, H. Kita, Airway exposure initiates peanut allergy by involving the IL-1 pathway and T follicular helper cells in mice. *J. Allergy Clin. Immunol.* **142**, 1144–1158.e8 (2018).
68. B. B. Cazac, J. Roes, TGF-β receptor controls B cell responsiveness and induction of IgA in vivo. *Immunity* **13**, 443–451 (2000).
69. A. R. Albright, J. Kabat, M. Li, F. Raso, A. Reboldi, J. R. Muppidi, TGFβ signaling in germinal center B cells promotes the transition from light zone to dark zone. *J. Exp. Med.* **216**, 2531–2545 (2019).
70. Y. Chung, S. Tanaka, F. Chu, R. I. Nurieva, G. J. Martinez, S. Rawal, Y.-H. Wang, H. Lim, J. M. Reynolds, X. Zhou, H. Fan, Z. Liu, S. S. Neelapu, C. Dong, Follicular regulatory T cells expressing Foxp3 and Bcl-6 suppress germinal center reactions. *Nat. Med.* **17**, 983–988 (2011).
71. H. C. Oettgen, T. R. Martin, A. Wynshaw-Boris, C. Deng, J. M. Drazen, P. Leder, Active anaphylaxis in IgE-deficient mice. *Nature* **370**, 367–370 (1994).
72. M. Martin, Cutadapt removes adapter sequences from high-throughput sequencing reads. *EMBnet.journal.* **17**, 10 (2011).
73. A. Dobin, C. Davis, F. Schlesinger, J. Drenkow, C. Zaleski, S. Jha, P. Batut, M. Chaisson, T. Gingeras, STAR: Ultrafast universal RNA-seq aligner. *Bioinformatics* **29**, 15–21 (2013).
74. B. Li, C. N. Dewey, RSEM: Accurate transcript quantification from RNA-Seq data with or without a reference genome. *BMC Bioinformatics.* **12**, 323 (2011).
75. M. I. Love, W. Huber, S. Anders, Moderated estimation of fold change and dispersion for RNA-seq data with DESeq2. *Genome Biol.* **15**, 550 (2014).
76. S. X. Ge, E. W. Son, R. Yao, iDEP: An integrated web application for differential expression and pathway analysis of RNA-Seq data. *BMC Bioinformatics.* **19**, 534 (2018).
77. V. K. Mootha, C. M. Lindgren, K. F. Eriksson, A. Subramanian, S. Sihag, J. Lehar, P. Puigserver, E. Carlsson, M. Ridderstråle, E. Laurila, N. Houstis, M. J. Daly, N. Patterson, J. P. Mesirov, T. R. Golub, P. Tamayo, B. Spiegelman, E. S. Lander, J. N. Hirschhorn, D. Altshuler, L. C. Groop, PGC-1α-responsive genes involved in oxidative phosphorylation are coordinately downregulated in human diabetes. *Nat. Genet.* **34**, 267–273 (2003).
78. A. Subramanian, P. Tamayo, V. K. Mootha, S. Mukherjee, B. L. Ebert, M. A. Gillette, A. Paulovich, S. L. Pomeroy, T. R. Golub, E. S. Lander, J. P. Mesirov, Gene set enrichment analysis: A knowledge-based approach for interpreting genome-wide expression profiles. *Proc. Natl. Acad. Sci.* **102**, 15545–15550 (2005).
79. H. Zeng, S. Cohen, C. Guy, S. Shrestha, G. Neale, S. A. Brown, C. Cloer, R. J. Kishton, X. Gao, B. Youngblood, M. Do, M. O. Li, J. W. Locasale, J. C. Rathmell, H. Chi, mTORC1 and mTORC2 kinase signaling and glucose metabolism drive follicular helper T cell differentiation. *Immunity* **45**, 540–554 (2016).
80. S. Dell'Orso, A. H. Juan, K. D. Ko, F. Naz, J. Perovanovic, G. Gutierrez-Cruz, X. Feng, V. Sartorelli, Correction: Single cell analysis of adult mouse skeletal muscle stem cells in homeostatic and regenerative conditions (doi: 10.1242/dev.174177). *Development* **146**, dev181743 (2019).
81. S. Horiuchi, H. Wu, W. C. Liu, N. Schmitt, J. Provot, Y. Liu, S. E. Bentebibel, R. A. Albrecht, M. Schotsaert, C. V. Forst, B. Zhang, H. Ueno, Tox2 is required for the maintenance of GC T_{FH} cells and the generation of memory T_{FH} cells. *Sci. Adv.* **7**, eabj1249 (2021).
82. K. J. Livak, T. D. Schmittgen, Analysis of relative gene expression data using real-time quantitative PCR and the 2−ΔΔCT Method. *Methods* **25**, 402–408 (2001).

Acknowledgments: We attest that the environment in which this work was conducted strives to be diverse and inclusive for all, particularly the underserved and underrepresented. **Funding:** This work was funded by the Division of Intramural Research, NIAID, NIH. **Author contributions:** Data collection: T.T.H., K.A.W., Z.S., J.L., M.T., L.L., and P.S. Data analysis: T.T.H., K.A.W., Z.S., D.M.S., C.Y., J.L., K.L., and P.A.F.-G. Conceptualization: T.T.H., K.A.W., K.L., and P.A.F.-G. Writing—original draft: T.T.H. and P.A.F.-G. Writing—review and editing: All authors provided writing edits. **Competing interests:** D.M.S. provides anonymized paid consultations about general scientific material through Guidepoint Consulting. All other authors declare that they have no competing interests. **Data and materials availability:** All materials are available upon request and material transfer agreement filing. Data have been deposited to GEO (GSE201463 and GSE203379) for public access as stated in Materials and Methods. All data needed to evaluate the conclusions in the paper are present in the paper or the Supplementary Materials.

Submitted 26 January 2023
Accepted 15 November 2023
Published 19 January 2024
10.1126/sciimmunol.adg8691